SOLAR HEATING & COOLING PROGRAMME
INTERNATIONAL ENERGY AGENCY

Task 38
Solar Air-Conditioning and Refrigeration

Exergy Analysis of Solar Cooling Systems

A technical report of subtask C3

Date: June 2010

Coordinator of Subtask C3 : LUIGI MARLETTA. University of Catania - Italy

Report edited by LUIGI MARLETTA

Contributors

Constanze Bongs	**Fraunhofer ISE, Heidenhofstr. 2, 79110 Freiburg, Germany**
Paul Bourdoukan	**SORANE, S.A, Rte du Bois, CP 248, 1024 Ecublens, Suisse**
Gianpiero Evola	**Industrial Engineering Dept. , University of Catania - Italy**
Patrice Joubert	**LEPTIAB, Université La Rochelle, Avenue Michel Crépeau, 17000 La Rochelle**
Luigi Marletta	**Industrial Engineering Dept. , University of Catania - Italy**
Harald Moser :	**Graz University of Technology, Institute of Thermal Engineering Inffeldgasse 25 B, A-8010 Graz**
Michel Pons	**LIMSI, CNRS-LIMSI, BP 133, Rue J. von Neumann, F-91403 Orsay Cedex, France**
René Rieberer	**Graz University of Technology, Institute of Thermal Engineering Inffeldgasse 25 B, A-8010 Graz**
Etienne Wurtz	**LOCIE, Université de Savoie, Campus Scientifique 73377 Le Bourget du Lac**

Table of Content

Introduction

Within the Task 38, the Subtask C was devoted to the Thermodynamic Analysis of solar cooling systems. Out of the many contributions offered by the participants, those ones collected in this Report are the most representative of the research activity carried out by the whole Group in the field of the exergy analysis and its applications to solar cooling.

By going through the paper, the Reader can recognize that for detecting the drawbacks of thermodynamic nature of energy engineering systems, the exergy approach is a more useful and powerful tool than energy analysis. Indeed, while the energy approach is based solely on the First Law, exergy analysis is founded on the combination of both the First and Second Law of Thermodynamics, thus offering a wider and more rational basis for investigation.

As a result, on the basis of the exergy assessment, it is possible to detect the distribution of irreversibility among the plant components, pinpointing those contributing most to the overall plant inefficiency and thus providing valuable information for system improvement and optimization.

The content of this Report is made of four contributions.

The first one by L. Marletta, is an overview of the exergy method, with fundamentals concepts and formulas.

In the second one, L. Marletta and G. Evola offer the exergy analysis of a DEC systems in comparison with and equivalent HVAC conventional system for air-conditioning, and show how chemical dehumidification and solar energy can help to obtain much better results both in terms of energy and exergy point of view.

Paul Bourdoukan with Patrice Joubert, Michel Pons and Etiewnne Wutz report on the exergy analysis of the Air-handling Unit (AHU) of a DEC system, based on experimental data.

Harald Moser contributes a paper dealing with the entropy analysis of an ammonia-water chiller for solar cooling applications, with a detailed picture of irreversibility distribution within the system and showing possible ways to improvement.

Constanze Bongs focuses the analysis on the very promising ECOS system, a sorptive heat exchanger able to perform simultaneously cooling and dehumidification of air streams.

Finally Michel Pons contributes a paper of more fundamental tenor, which discusses the reference conditions to adopt in the exergy analysis of systems experiencing variable environmental temperature.

1 Exergy analysis. A few hints (Luigi Marletta)

- Energy analysis

When dealing with energy balances, we usually refer to the first law of Termodynamics, which states that energy is a conservative property; this means that during any real steady-state process the overall energy flow leaving a system equals the overall energy flow entering the system, Fig. 1.

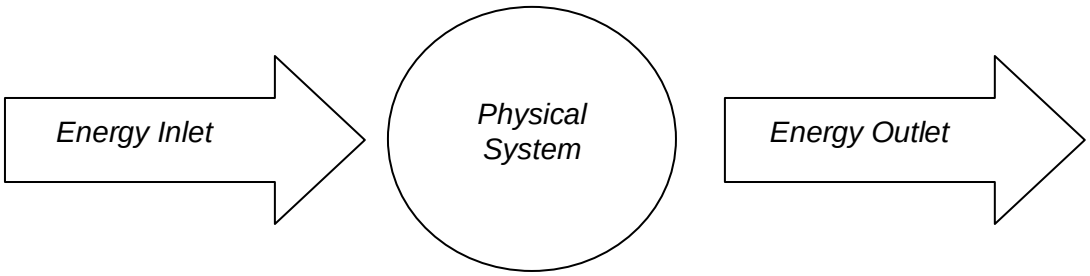

Fig. 1. Energy flows across a physical system

Actually, the different forms of energy (thermal, mechanical, internal, potential, kinetic) may individually undergo quantitative changes, but the overall amount of energy is conserved. The energy balance equation, which quantifies the energy conservation law for a stationary process observed through a control volume, may be stated as follows:

$$\dot{Q} - P = \sum_{outlet} \dot{m}_k \left(h + gz + \frac{w^2}{2} \right)_k - \sum_{inlet} \dot{m}_k \left(h + gz + \frac{w^2}{2} \right)_k \tag{0.1}$$

where:

$\dot{Q}$ = thermal energy flow crossing the system boundaries (W);

P = mechanical power crossing the system boundaries (W);

$\dot{m}$ = mass flow rate entering / leaving the system (kg/s);

z = height of the system above a reference level (m);

w = mass flow velocity (m/s).

h = specific enthalpy measured at the system inlet and outlet (kJ/kg)

The index of performance derived from such an approach compares the amount of energy required by the final user (either electric, or mechanical, or thermal…) to the total amount of energy exploited by the system, expressed as:

Energy efficiency: $\eta = \dfrac{\text{Energy released to the user}}{\text{Energy provided to the system}}$

One must realize that such a definition compares different forms of energy. As an example, in the case of a power plant for the production of electric energy, the energy efficiency is defined as:

$$\eta = \frac{P}{Q_{th}} \tag{0.2}$$

where P is the electric power, and Q_{th} the thermal energy to drive the system.

But, as a matter of fact, different forms of energy have different potentials to produce useful work. So the definition of efficiency stated above is a comparison between quantities which are metrically homogeneous but *not* conceptually equivalent.

- The Second Law of Thermodynamics

The *Second Law of Thermodynamics* may help overcome this drawback, on the basis of a rather different approach to system analysis.

The starting point is that real processes are not reversible and give rise to entropy production: friction, hysteresis, molecular or thermal diffusion are the most common examples of irreversibilities occurring in a real process. The mathematical form of the Second Law most suitable for our purposes is the *Clausius* equation:

$$\sum_{outlet} (\dot{m} \cdot s)_k - \sum_{inlet} (\dot{m} \cdot s)_k = \sum_j \left(\frac{\dot{Q}}{T} \right)_j + \sigma \tag{0.3}$$

where: s = entropy per unit mass (kJ/(kg·K));

$\dot{Q}$ = heat transfer occurring through the system boundaries (W);

T = temperature of the environment being involved in the heat transfer (K);

σ = overall entropy production due to irreversibility (W/K).

The reader is reminded that, as stated by the Second Law, $\sigma \geq 0$, being $\sigma = 0$ only for ideal (reversible) processes.

This relationship is precious to us, as it allows the assessment of entropy production σ, which is always the unknown of the problem.

It is intuitive that when dealing with complex systems, it is possible to decompose them into several, more simple subsystems; by evaluating σ for each one of them, it is possible to detect the ones most responsible for thermodynamic drawbacks and thus provide corrective measures.

- The Gouy-Stodola equation

Let us realize that the first law contains a term for work, but no term for irreversibility, whereas the second law contains a term for irreversibility but not for work.

In order to state a more general equation than the previous ones, let us combine the first and the second law statements. Before doing this it is appropriate to adopt the following expressions:

$$Q = Q_o + \sum_j Q_j$$
$$\frac{Q}{T} = \frac{Q_o}{T_o} + \sum_j \frac{Q_j}{T_j} \qquad (0.4)$$

Q_o being the heat transfer to the environment and T_o its temperature.

By combining equations (0.1) and (0.3) and taking into account eq. (0.4), one obtains the Gouy-Stodola equation:

$$P = \sum_{\mathrm{n}} \dot{Q}_n \cdot \left(1 - \frac{T_o}{T_n}\right) + \sum_{\mathrm{Inlet}} \dot{m}_k \left(h - T_o s + \frac{w^2}{2} + g\,z\right)_k - \sum_{\mathrm{Outlet}} \dot{m}_k \left(h - T_o s + \frac{w^2}{2} + g\,z\right)_k - T_o \sigma \qquad (0.5)$$

For an ideal *reversible* process (σ = 0), the *Gouy-Stodola* equation yields:

$$P_{id} = \sum_{\mathrm{n}} \dot{Q}_n \cdot \left(1 - \frac{T_o}{T_n}\right) + \sum_{\mathrm{Inlet}} \dot{m}_k \left(h - T_o s + \frac{w^2}{2} + g\,z\right)_k - \sum_{\mathrm{Outlet}} \dot{m}_k \left(h - T_o s + \frac{w^2}{2} + g\,z\right)_k \qquad (0.6)$$

For all real processes σ > 0, thus $P_{id} > P$, in other terms

$$P_{id} - P = \sigma T_o > 0 \qquad (0.7)$$

This means that irreversibilities erode the thermodynamic potential of the energy flows; in other words, at the end of the process or at the system outlet, the energy flows have a lower potential to produce work, and this reduction is measured by the entropy production σT_o. This term is also referred to as “Irreversibility”:

$$I = \sigma T_o$$

- The dead state

The work potential of a system at a given state may be assessed by letting the system proceed towards and actually reach a stable equilibrium with the environment. In fact, when the system and the environment are in equilibrium, no further change of state can occur spontaneously and hence no further work can be produced.

When such a situation occurs, the system is said to be in the *dead state*. Specifically the dead state is characterized by conventional values for pressure p_o and temperature T_o. Additional requirements for the dead state are that the velocity of the fluid stream is zero ($w_o = 0$) and the gravitational potential energy is zero ($z_o = 0$). These restrictions of pressure, temperature, velocity and elevation characterize the *restricted dead state*, associated with

the thermomechanical equilibrium with the environment. It is restricted in the sense that the chemical equilibrium with the environment is not considered, that is the control mass is not allowed to pass into or react chemically with the environment.The problem of the chemical equilibrium with the environment will be dealt with later on.

- The concept of Exergy

Exergy is defined as the work potential of a system relative to its dead state.

Following this definition, for each term appearing in eq.(0.5), it is possible to derive an expression for exergy. So we have :

Exergy of (mechan. or electrical) work *P*: $E_P = P$

Exergy of heat *Q* available at temp. *T* : $E_Q = Q(1-\frac{T_o}{T})$

Exergy of a mass flow: $E_m = \dot{m}\left[(h-h_o)-T_o(s-s_o)+\frac{w^2-w_o{}^2}{2}+g(z-z_o)\right]$

So for a control volume, eq.(0.5) may be rewritten in terms of exergy, as follows :

$$(E_P)_{out}-(E_P)_{in}=(E_Q)_{in}-(E_Q)_{out}+(E_m)_{in}-(E_m)_{out}-\sigma T_o$$

and rearranging the terms:

$$(E_P+E_Q+E_m)_{in}=(E_P+E_Q+E_m)_{out}+\sigma T_o$$

Therefore:

$$\sigma T_o=\sum_{in} E_j-\sum_{out} E_k \qquad (0.8)$$

The irreversibility can then be quantified as the difference in exergy measured at the inlet and outlet sections of the control volume.

- Exergy and Anergy

Let us consider a given amount of thermal energy *Q* available at the temperature *T.* Thus :

$$E_Q=Q\left(1-\frac{T_o}{T}\right)$$

E_Q can be thought of as the maximum work which can be extracted from a Carnot cycle, receiving the heat Q and working between the temperatures T and T_o .

By rewriting the equation in the form:

$$E_Q = Q - \frac{T_o}{T} Q$$

it is easy to recognize Q as the amount of energy available at the beginning, and $Q \cdot (T_o/T)$ as the amount of energy rejected to the environment as thermal waste; at these conditions, energy is no longer recoverable for technical purposes. Some Authors refer to this quantity as "not available energy" or *Anergy*.

Similar considerations can be made in relation to the mass flow, where:

The exergy is: $$(h - h_o) - T_o(s - s_o) + \frac{w^2 - w_o{}^2}{2} + g(z - z_o)$$

The energy is: $$(h - h_o) + \frac{w^2 - w_o{}^2}{2} + g(z - z_o)$$

The anergy is: $$T_o(s - s_o)$$

All forms of energy at the dead state are anergy. The natural environment is an infinite reservoir of anergy. Distinction should be made between anergy and irreversibility. The former has always existed, the latter results while a process is occurring. Irreversibility is anergy which arises whenever a physical event takes place.

Anergy may enter the control volume and then grow by addition of the irreversibilities. Eventually the anergy flow will join the irreversibility flow, so that at the system outlet the anergy results higher than it was at the inlet.

To summarize the previous results, the following relationship can be stated between energy, exergy and anergy :

Energy = Exergy + Anergy

A pictorial view of the concepts outlined so far is provided in Fig. 2. Its message is clear: going through the physical system, the exergy flow is lowered by the entropy production, the anergy flow increases by the same quantity, while the energy flow remains constant.

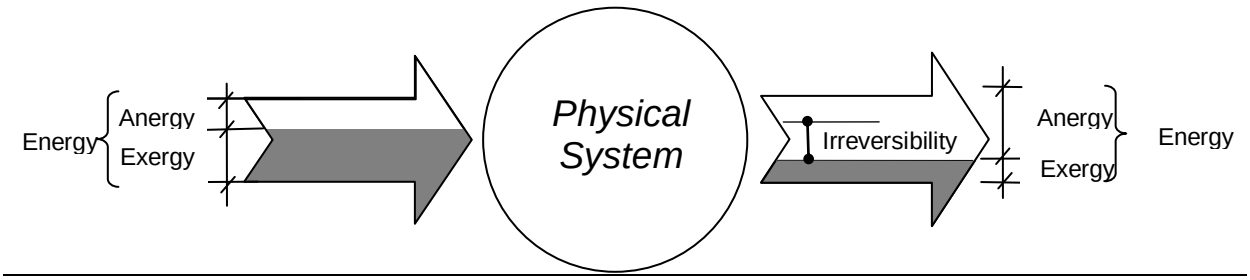

Fig. 2. Exergy and anergy flows across a physical system

In conclusion, by using the exergy and anergy concepts, the first and second law of thermodynamics may be reformulated as follows:

1. in any process the sum of exergy and anergy remains constant
2. in any *real* process the exergy decreases and the anergy increases by the same quantity as the entropy production.
3. The anergy cannot be converted into exergy

- Exergy efficiency

According to this approach, the thermodynamic figure of merit for a process in a second law perspective is the exergy efficiency, defined as:

$$\textbf{\textit{Exergy Efficiency}}: \quad \zeta = \frac{\text{Exergy}\,OUTPUT}{\text{Exergy}\,INPUT}$$

In formulas:

$$\zeta = \frac{E_{out}}{E_{in}} = \frac{E_{in} - \sigma T_o}{E_{in}} = 1 - \frac{\sigma T_o}{E_{in}}$$

The exergy efficiency is thus a ratio between quantities that now are both metrically *and* conceptually homogeneous. The numerical values of ζ never exceed unity. The maximum exergy efficiency (ζ =1) is only achievable by ideal systems (σ = 0).

In order to perceive how different the exergy approach is from the energy approach, and how surprising the results are sometimes, the problem of heating and cooling will be discussed in the following section in a very basic way.

ENERGY EFFICIENCY vs EXERGY EFFICIENCY in short.

Energy efficiency	Exergy efficiency
• Takes into account only the 1.st Law • Compares metrically but *not always* conceptually homogenous terms	• Takes into account the 1.st and 2.nd Law • Compares metrically *and* conceptually homogenous terms

• Is always $\eta > 0$
  ○ but in some cases is $\eta > 1$ (Inverse cycles, heat pumps…)
	• Is always $1 > \zeta > 0$
	  ○ without exceptions

Applications of exergy analysis to solar cooling systems

2. Exergy analysis of a solar DEC (Luigi Marletta, Gianpiero Evola)

- Premises

The "available energy" (availability) of a mixture of substances at a given temperature and pressure (*T, p*) is the maximum work obtainable by bringing the stream to the thermo-mechanical equilibrium with the environment. For systems where the mass is not allowed to pass into or chemically react with the environment, the achieved perfect and stable equilibrium is referred to as the *restricted dead state*.

When processes have a mass interaction with the environment, in the sense that the mass may be released to the environment and/or have chemical reactions with it, then it is necessary to take into account the chemical potential of the constituents, since it is different from that of the environment. After reaching the mechanical, thermal *and chemical* equilibrium with the environment, the system is said to be in the *ultimate dead state*.

The chemical equilibrium involves the calculation of the chemical potential of substances and an extensive theoretical treatment, which can be seen from the specialized literature.

The operative formula for the "*available energy*" of a humid air stream, as a binary mixture of dry air and water vapour, was first stated by Wepfer, Gaggioli and Obert in a fundamental article published in 1979, as a function of pressure *p,* temperature *T*, and absolute humidity *x*:

$$e_a = e(T, x, p) = (c_{pa} + x \cdot c_{pv})(T - T_o - T_o \ln \frac{T}{T_o}) + (1+\bar{x}) R_a T_o \ln \frac{p}{p_o} + R_a T_o \left[(1+\bar{x}) \ln \frac{1+\bar{x}_o}{1+\bar{x}} + \bar{x} \ln \frac{\bar{x}}{\bar{x}_o} \right]$$

where: $\bar{x} = x / 0.622$, c_{pa} and c_{pv} are the specific heat for the dry air and water vapour respectively and R_a the gas constant for the dry air. In real cases $p \cong p_o$, thus $e_a = e(T,x)$.

The reference condition (*ultimate dead state*), denoted with the subscript "$_o$" is usually assumed to be that of outdoors; therefore: $x_o = x_E$; $T_o = T_E$; $p_o = p_E$; $e_E = e_o = 0$.

The exergy of a water flow rate, when kinetic and potential terms can be disregarded, reduces to:

$$e_w = c_{pw}(T - T_o) - T_o c_{pw} \ln \frac{T}{T_o} - R_v T_o \ln \phi_o \qquad (0.9)$$

where c_{pw} is the specific heat for liquid water, R_v the water vapour constant and ϕ_o the relative humidity for the reference state ($\phi_o = \phi_E$) .

The exergy of the condensate produced by saturating the vapour contained in the humid air can be expressed as a function of the relative humidity ϕ_o of the outdoor air:

$$e_c = - R_v T_o \ln \phi_o$$

By using these formulas and the *Gouy-Stodola equation,* it is possible to study the basic processes of the air conditioning under a second law perspective.

In the following sections two worked examples will be carried out, i.e. 1.) an all air HVAC system for summer operation, and 2.) an air conditioning system, based on Desiccant rotors and Evaporative Cooling (DEC). The two systems will be compared under the assumption of the same inlet conditions and mass flow rate of the supply air.

This investigation will allow us to: 1. perceive the difference between the energy and exergy approach and 2. acknowledge that the latter provides very often more valuable information than the former for the improvement of energy systems.

- The HVAC Reference design

To start this analysis with a simple example, let us consider the HVAC in summer operation reported in Fig. 3 in terms of plant layout and psychrometric processes.

It is an all air system (i.e. without air recirculation), where the sensible (Q_S) to total load (Q_T) ratio is taken to be $R=Q_s/Q_T= 0.75$. Under this assumption, suitable inlet conditions are those of state (I). The air mass flow rate is assumed to be m_a=1 kg/s. The reference conditions are reported in Tab. 1.

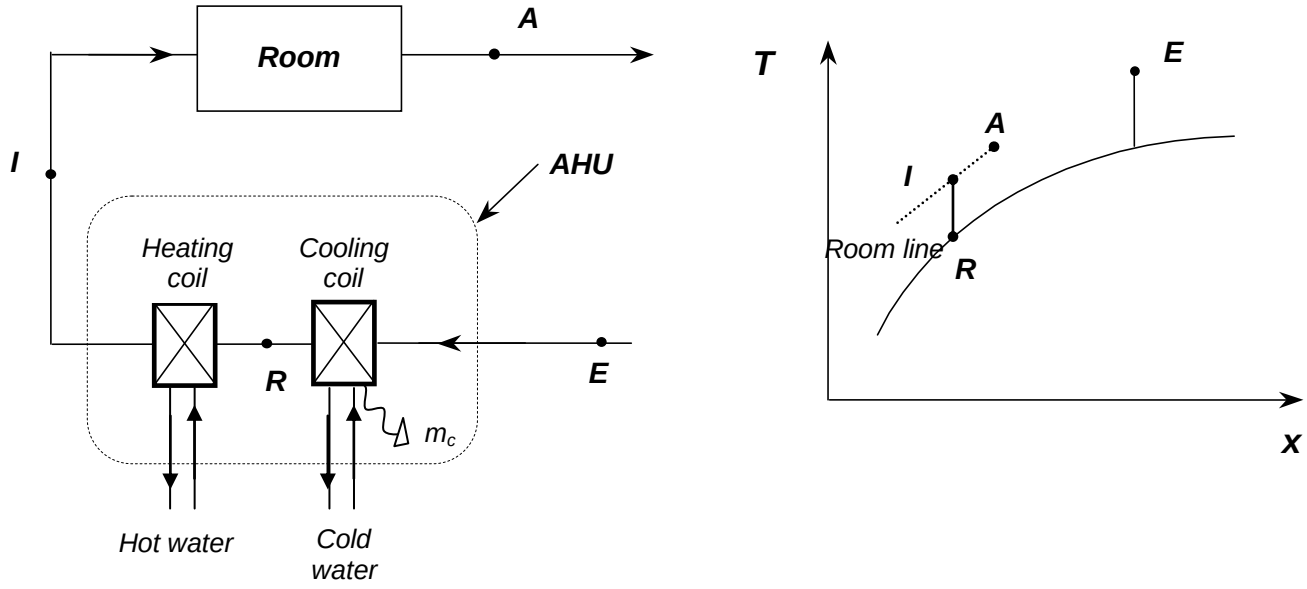

Fig. 3. Plant lay-out and thermal cycle in the psychrometric chart of a HVAC

Tab. 1

	T (°C)	x (g/kg)
A	26	10.5
E	35	21.4
I	18.5	9.5
R	13.3	9.5

The exergy analysis of the Air-Handling Unit can be conducted according to approach outlined above and the results presented in the form of an exergy-anergy flow diagram, as shown in Fig. 4 .

From this picture it can be seen that the irreversibility production is most attributable to the cooling and dehumidification process, a lot to the exhaust (air and condensate) and the rest to the re-heating process.

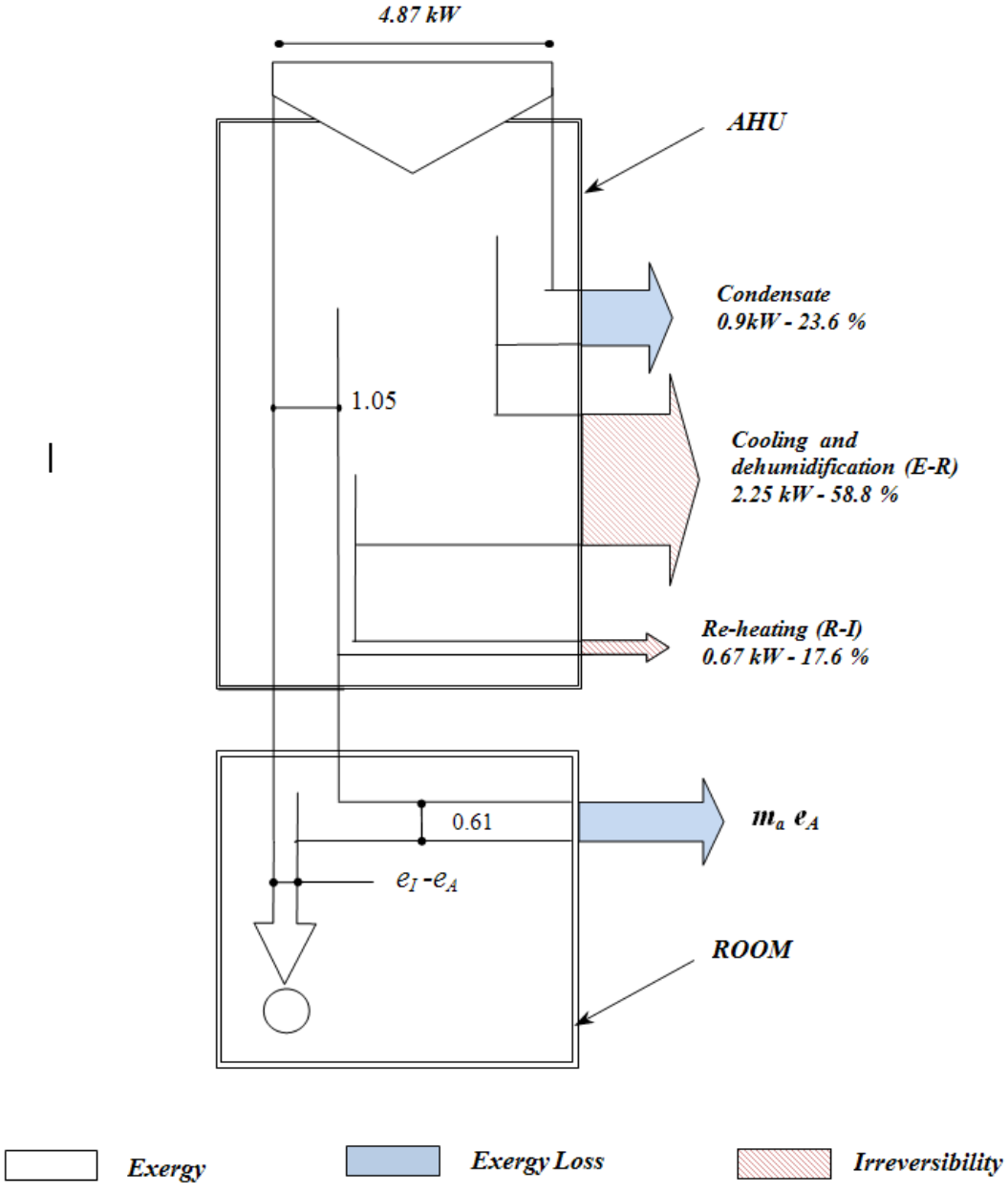

Fig. 4. Exergy-Anergy flow diagram for the Air-Handling Unit

- Energy and Exergy Analysis of the overall HVAC

In order to assess the Primary Energy consumption and the related exergy content for the plant as a whole, let us enlarge the control volume so as to include the power technologies, i.e. the boiler (BL) and the chiller (CL), as shown in Fig. 5.

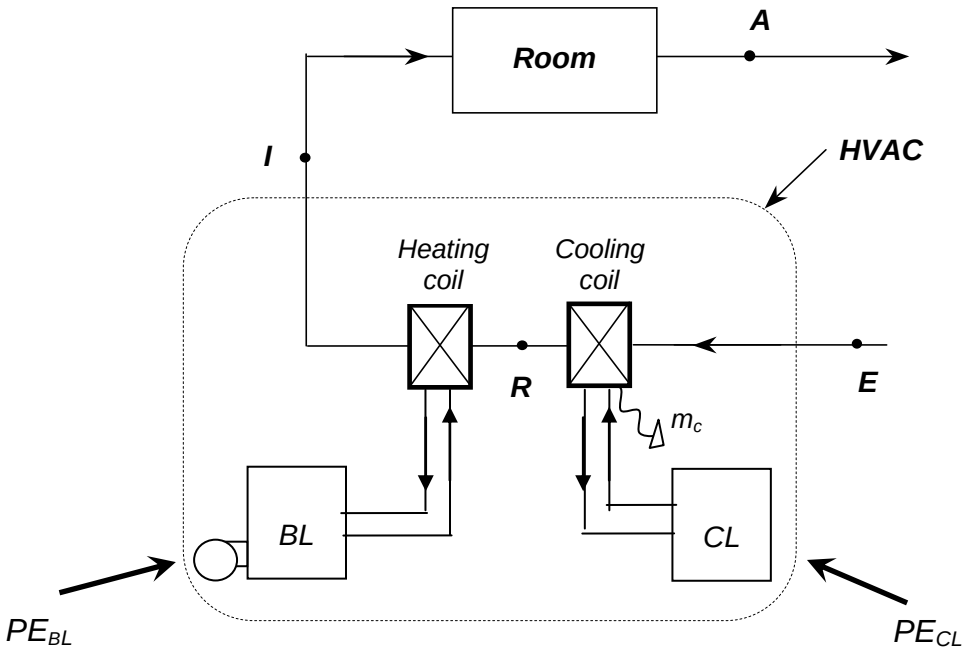

Fig. 5. Control volume for the overall HVAC

It is not the case to go into details here for the calculation of the Primary Energy (PE) consumption, related to chiller and boiler. The problem here is how to convert PE (usually referred to the lower heating value of fuels) into exergy. To this aim we may adopt a corrective factor ψ which can be taken form literature [1] [2], or (in case of lack of data) assessed as the higher (H_s) to lower heating value (H_i) ratio for a given fuel or mix of fuels:

$$\psi = \frac{H_s}{H_i}$$

So, for a boiler fed with natural gas and the central power stations based on a nationwide mix of fuels where oil is dominant, we could assume:

$$\psi_{BL} = \left(H_s / H_i\right)_{BL} \cong 1.1 \qquad \psi_{el} = \left(H_s / H_i\right)_{el} \cong 1.06$$

At the end, the exergy content of a given PE rate can be assessed as the product (PE ψ). The exergy analysis, extended up to include the energy sources, gives rise to the flow diagram in Fig. 6.

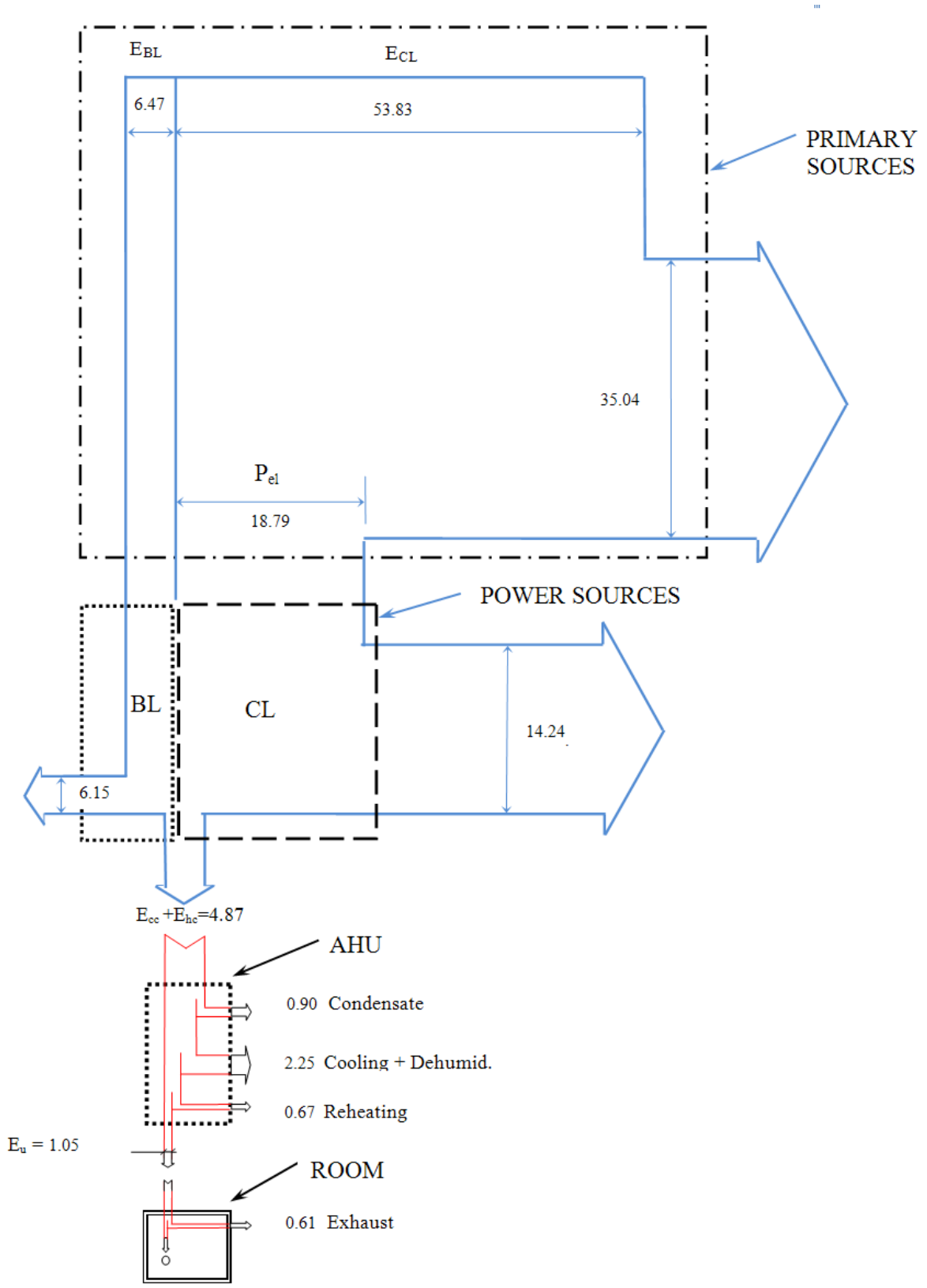

Fig. 6 Exergy-Anergy flow of the HVAC as a whole

➢ Definitions of thermodynamic indexes

The thermodynamic performance of energy engineering system considered in this study will be judged on the basis of the following indexes:

- SPEC: Specific Primary Energy Consumption (kW/kW)
  defined as the primary energy comsumption per unit of useful energy (heat, cool or mechanical energy).
- SPIR: Specific Irreversibility Production (kW/kW)
  defined as the irreversibility production per unit of useful energy (heat, cool or mechanical energy).

- ζ_{AHU} : exergy efficiency of the Air Handling Unit (AHU)
  defined as the ratio of net exergy output (supply air) to the net exergy input to the AHU, excluding the exergy power sources (boiler and chiller)
- ζ_{PS} : exergy efficiency of the Power Sources Unit (PS)
  defined as the ratio of net exergy output (working fluids leaving heating and cooling coils) to the net exergy input to the AHU (exergy of heat and electricity)

- ζ : exergy efficiency of the overall system.
  defined as the net exergy output (supply air) to the net exergy input to the overall system (exergy of primary sources).

➢ Exergy evaluation of the HVAC

The thermodynamic indexes defined above, for the AHU and the HVAC system as a whole, are collected in Tab. 2

Tab. 2

SPEC (kW/kW)	5.6
SPIR (kW/kW)	5.9
ζ_{AHU}	21.5 %
ζ_{PS}	8.10 %
ζ	1.74 %

Beside the concept, outlined in the previous section, that the most responsible process for the exergy destruction in the AHU is cooling and dehumidification, the important message which arises from these results is about the energy sources.

The poor exergy efficiency of the power sources, ζ_S = 8.1 % means that their thermodynamic potential is much higher than that required by the end uses. This can be understood by referring, for example, to the exergy offered to the boiler (E_{BL}=6.47 kW) compared to that found in the hot water stream (E_{in_hc}=6.47-6.15=0.32 kW), which parallels

the distance between the flame temperature in the boiler (T_f =1500K) and that required to produce hot water (60°C), not to mention the final air stream re-heating temperature (T_l=18.5°C).

Things get even worse if we look at the cooling process. To obtain a cold water flow with an exergy content E_{in_cc}=4.55 kW, we spend as much exergy as E_{CL}=53.83 kW.

Only 8.10 % of this amount is entering the AHU and, out of it, only 21,5% (ζ_{AHU} = 21.5%) is in turn being converted into useful exergy E_u, resulting in an overall exergy efficiency as low as ζ=1.74%.

A first conclusion is that sources with high energy potential as compared to that required by the final uses, should be used as little as possible, and particularly electricity.

In order to overcome these problems, it is natural to look for more appropriate technologies.

In the subsequent sections we will investigate if chemical dehumidification instead of mechanical compression cooling systems and solar energy instead of conventional energy technologies based on combustion processes, may help to this end.

- DEC System description

The plant scheme adopted for this study and the corresponding thermal cycle are shown respectively in Fig. 7 and Fig. 8. The cycle is differs slightly from that usually mentioned in Literature [10] , in order to match the outdoor conditions of the Mediterranean area, where relative humidity is more likely 60% than 40%. That implies the introduction of a chiller to operate a pre-cooling before the air stream enters the desiccant wheel. As a result, the system under examination is made by an Air-Handling Unit (AHU) based on a solid desiccant wheel, provided with a rotary heat exchanger and a spray humidifier for evaporative cooling.

- Operative conditions

The psychrometric conditions for every point of the thermal cycle are reported in Tab. 3 whereas Tab. 4 shows the inlet and outlet conditions of the water to the heating and cooling coil. The regeneration airflow rate is assumed equal to that of the supply air, thus m_a= m_{reg} = 1 kg/s. A regeneration temperature T_G = 80°C has been assumed; the exergy values of air and water flows are assessed according to the definitions and formulas mentioned in the previous sections.

- First results

In Fig. 9 the results of the exergy analysis, conducted on the AHU, are given in the pictorial form of an exergy-anergy flow diagram. The picture clearly shows that most of the exergy is destroyed by irreversibility and converted into anergy, so that the exergy efficiency of the whole system is as low as 16.42%. (=1.05/ (0.61+0.23+4.1+0.87+0.64) =0.1642). The components most responsible for the irreversibility production are the heating coil (26.9%), the heat recovery wheel (26.9%) , the desiccant wheel (25%) and the cooling coils (8.6+7.7=16.3 %). All that tell us about the improper use is made of the energy sources, in

the sense that the thermodynamic potential used to drive processes is usually much higher than that required by the end uses.

A first strategy for improvement may be that of reducing the regeneration temperature. That would decrease one of the most important contributions to the irreversibility production, such as the heat source represented by the heating coil.

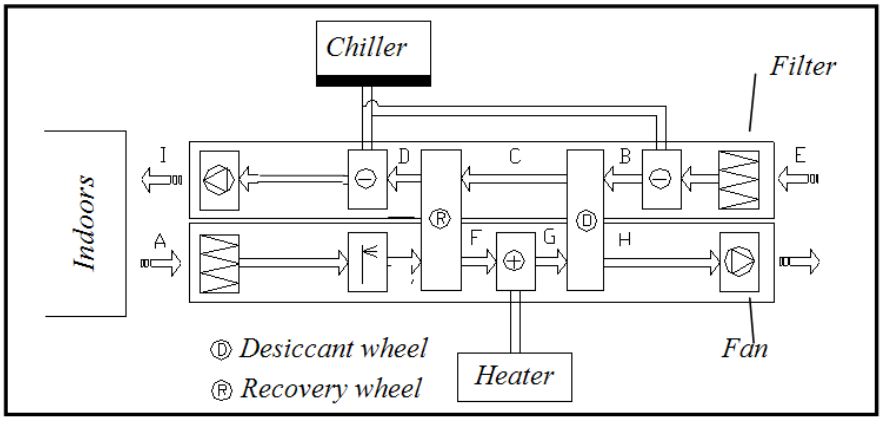

Fig. 7. Lay-out of an Air-Handling Unit with a desiccant wheel

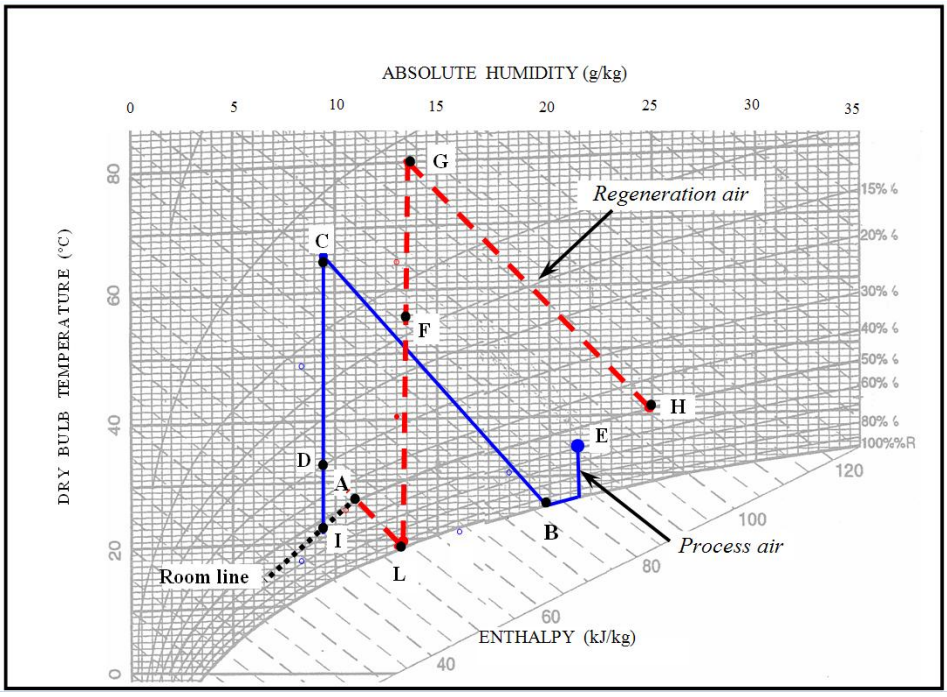

Fig. 8. Thermal cycle of DEC in the psychrometric chart

	A	B	C	D	E	F	G	H	I	L
t (°C)	26.0	25.7	65.4	32.7	35.0	51.4	80.0	40.5	18.5	18.7
x(g/kg)	10.5	21.0	9.5	9.5	21.4	13.5	13.5	25.0	9.5	13.5

Tab. 3: Psychrometric conditions for the open-cycle desiccant system.

	Cooling coil	***Heating coil***
Inlet	15 °C	90 °C
Outlet	20 °C	80 °C

Tab. 4: Water inlet and outlet conditions.

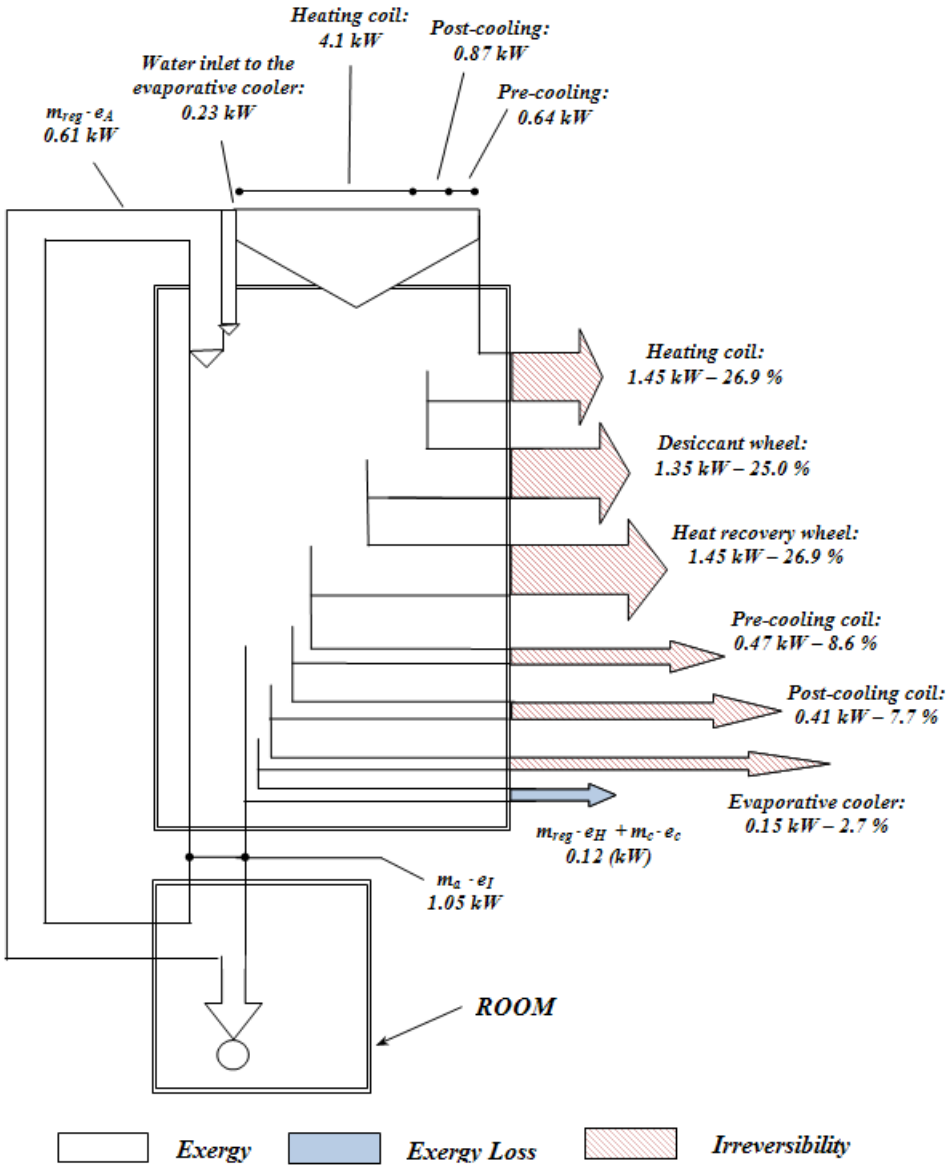

Fig. 9. Exergy-Anergy flow diagram for the AHU of a DEC

- Role of the regeneration temperature

To perceive the effect of the regeneration temperature on the exergy performance of a DEC, the computational procedure, followed above for T_{reg} = 80°C, was repeated for T_{reg} = 70°C and T_{reg} = 90°C.

Obviously, each case required the rearrangement of the whole cycle on the psychrometric chart and the adaptation of some data. The operating conditions for the three cases are summarized in Tab. 5. The results can be seen in Fig. 10 to Fig. 12.

As expected, reducing T_{reg} produces beneficial effects on the DEC in terms of irreversibility (Fig. 10). The most relevant ones are for the heat recovery and the desiccant wheel, although partially counterbalanced by an increase of irreversibility in the pre-cooling coil (as expected, due to the increasing need of pre-cooling and the decreasing effectiveness of the desiccant material).

The results of the analysis in Tab. 6 show that decreasing T_{reg} yields improvements in all the performance indexes (SPEC, SPIR, ζ_{AHU}, ζ). In any case, only the DEC with T_{reg} =70°C is the best one among all, as far as the overall exergy efficiency is concerned.

However it is interesting to assess the sensitivity of ζ_{AHU} and ζ to the T_{reg} ; that can be done by using data in Tab. 6. So, decreasing T_{reg} from 90°C to 70°C, one obtains:

$$\Delta \zeta_{AHU} = + 47.4\% \qquad \Delta \zeta = + 16.5\%$$

The message is that reducing T_{reg} is more beneficial for the AHU than for the whole system. Since in between there are the power sources (boiler and chiller, with related primary energy consumption), then to achieve substantial improvements for the whole system, we must look for energy sources more appropriate than those used so far.

In the next section we will see if solar energy can help to this end.

$T_{reg}=T_G$	T_B	x_B	T_C	x_C	T_D	x_D	T_F	x_F	T_H	x_H
70°C	24.5	19.5	57.9	9.5	30.5	9.5	46.1	13.5	36.6	23.5
80°C	27.5	21.0	65.4	9.5	32.7	9.5	51.4	13.5	40.5	25.0
90°C	28.9	21.4	72.1	9.5	34.7	9.5	56.0	13.5	46.8	25.4

Tab. 5. Operative conditions for various Regeneration Temperatures Treg

	HVAC	DEC 70°C	DEC 80°C	DEC 90°C
ζ_{AHU}	21.5%	19.6 %	16.2%	13.3%
ζ	1.74%	2.0%	1.8%	1.7%
SPIR (kW/kW)	5.9	5.2	5.6	6.2
SPEC (kW/kW)	5.6	4.8	5.1	5.5

Tab. 6. Relevant data for various T_{reg}.

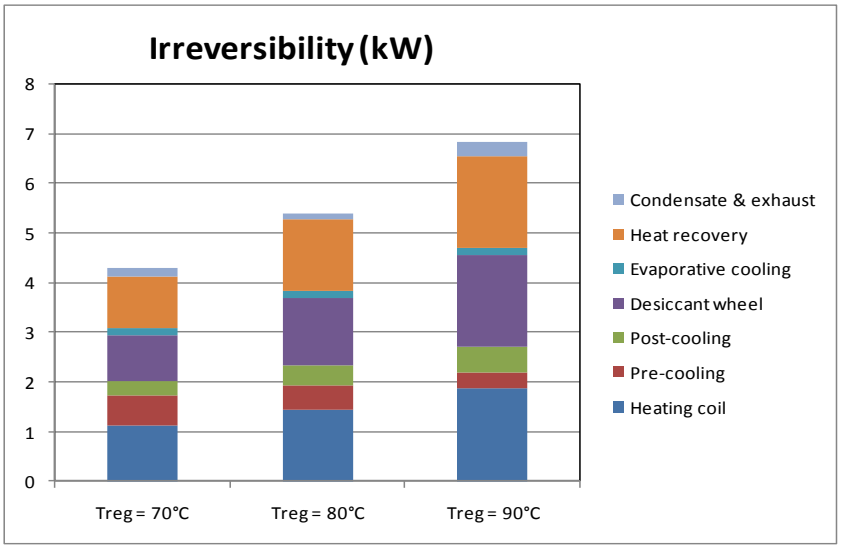

Fig. 10. Irreversibility (kW) in the AHU for each component and various T_{reg}

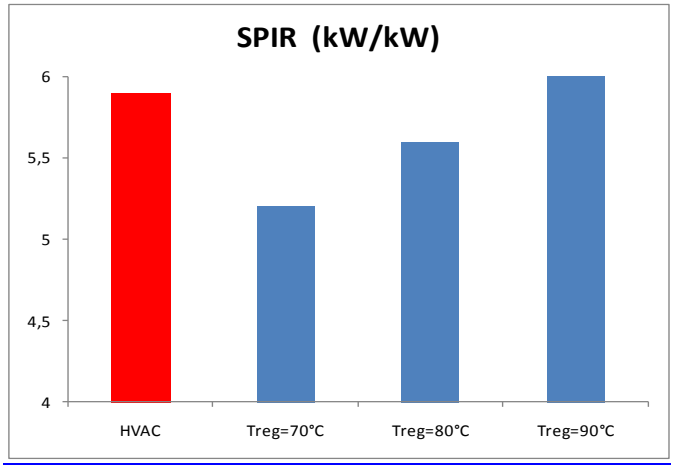

Fig. 11. Specific Irreversibility in the AHU for various T_{reg}

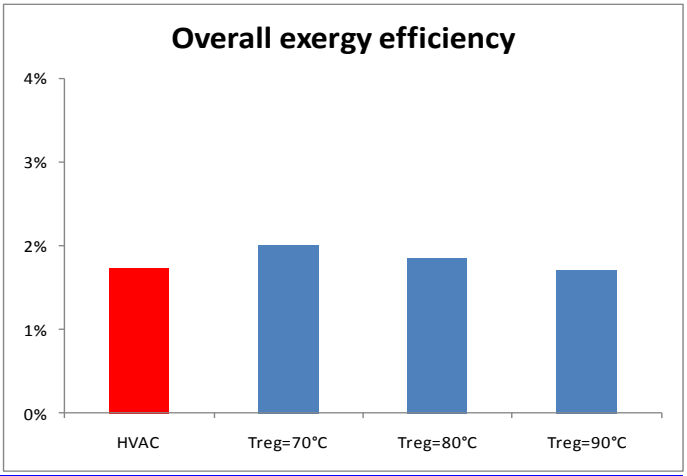

Fig. 12. Overal exergy efficiency for various T_{reg}

- Solar assisted desiccant systems (DEC)

To make the desiccant systems competitive with the conventional HVAC, it is suitable to use solar energy. For absorption based cooling systems, solar energy is being used as a thermal source to feed the chiller; in the case of a DEC system, it is used for regeneration purposes.

Because of the relatively low temperature required by modern desiccant wheels (70-80°C), flat-plate collectors can be used. Thus the only component "seen" by the solar section is the heating coil aimed at regenerating the desiccant wheel.

Usually not all the energy needs of the heating coil are matched by the solar source, but only a fraction *F* , the rest (*1-F*) being provided by some auxiliary source of heat, that here is assumed to be a conventional boiler.

As a result, in the following analysis, the energy/exergy performance of the solar DEC will be assessed as a function of *F* (the "solar fraction").

A necessary step in this analysis is the evaluation of exergy for a solar collector. To this end different methods are proposed in the literature.

In this context the exergy of the solar collector is assessed from the overall energy impinging on the collector (Q/η_{SC}), being η_{SC} the collector efficiency and Q the thermal energy required by the end-use (in our case the regeneration process of the desiccant material). This amount of energy is thought as offered to a Carnot cycle operating between the environmental temperature T_o and the highest temperature occurring in the collector, i.e. the plate temperature T_p. In this study: T_p = 80°C and η_{SC} =0.6.

In formula :

$$E_{SC} = \frac{Q}{\eta_{SC}}\left(1-\frac{T_o}{T_p}\right)$$

Thus the overall exergy efficiency of a DEC can be stated as follows:

$$\zeta(F) = \frac{m_a \cdot e_I}{m_{reg} \cdot e_A + E_{fw} + E_{CL} + E_{BL}(F) + E_{sol}(F)}$$

Clearly $m_a\ e_I$ is the exergy of the supply air stream, while the denominator includes the all the exergy input, provided through the regeneration air ($m_{reg}\ e_A$), the chiller (E_{CL}), the boiler (E_{BL}), the solar section (E_{sol}) and the feedwater to the evaporative cooler (E_{fw}).

- Energy and exergy analysis of a solar DEC

The most interesting results of the energy and exergy analysis of a solar DEC are summarized in (Fig. 13)**Errore. L'origine riferimento non è stata trovata.**. In each plot the straight line refers to the conventional HVAC considered above (COP=2.8).

As expected, the use of solar energy makes the SPEC decrease steadily, whatever is the solar fraction. This effect is enhanced by the regeneration temperature, in the sense that the lower the T_{reg} , the lower the SPEC. Actually, for the case under examination, this is true as long as *F* < 60%. For *F*>60% the lines cross each other: it means that a more effective dehumidification, due to a higher regeneration temperature, has a greater benefit than the energy savings due to a higher solar fraction.

But more importantly, while SPEC has a linear relationship with F, the overall efficiency ζ (Fig. 13) shows a steep increase with *F*: that proves solar energy to be a very appropriate source of exergy for this kind of applications.

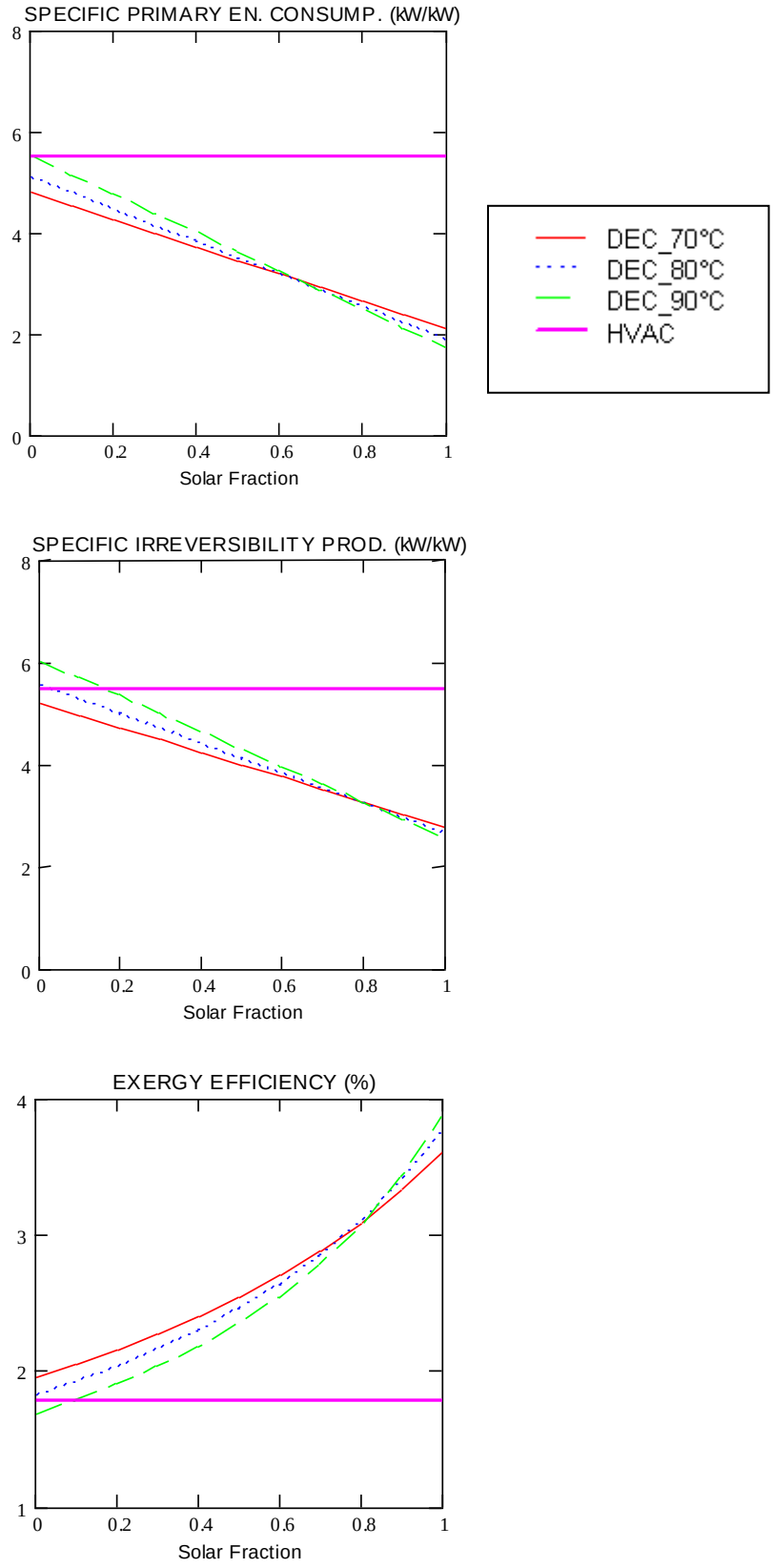

Fig. 13. Thermodynamic indexes for a solar DEC

- Improving the solar DEC

The performance of the solar DEC can be further improved by the introduction of an enthalpy wheel in the thermal cycle.

Enthalpy wheels look nearly like desiccants wheels. Both use desiccant materials impregnated into a support structure, usually shaped as a honeycomb open on both ends. The structure has the form of a wheel rotating through two separate air streams, with the first one dried by the desiccant and the second one (reactivation or regeneration air) heated to dry the desiccant.

The position of the enthalpy wheel in the plant lay-out is shown in Fig. 14 , while the thermal cycle is given in Fig. 15.

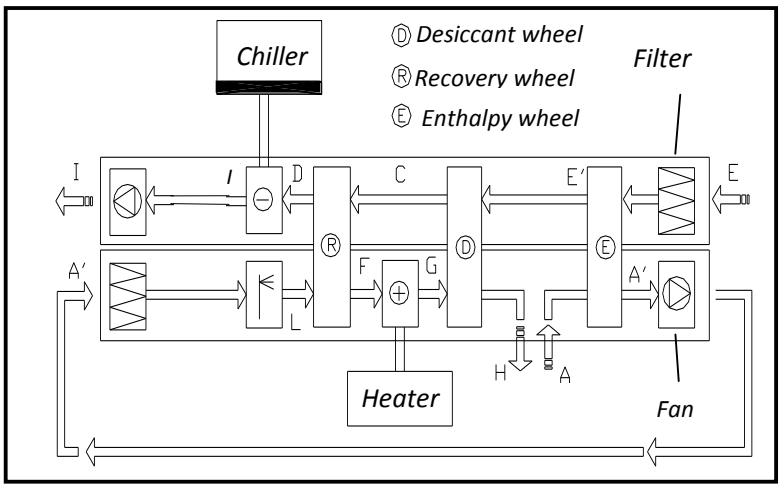

Fig. 14. Solar DEC lay-out with enthalpy wheel

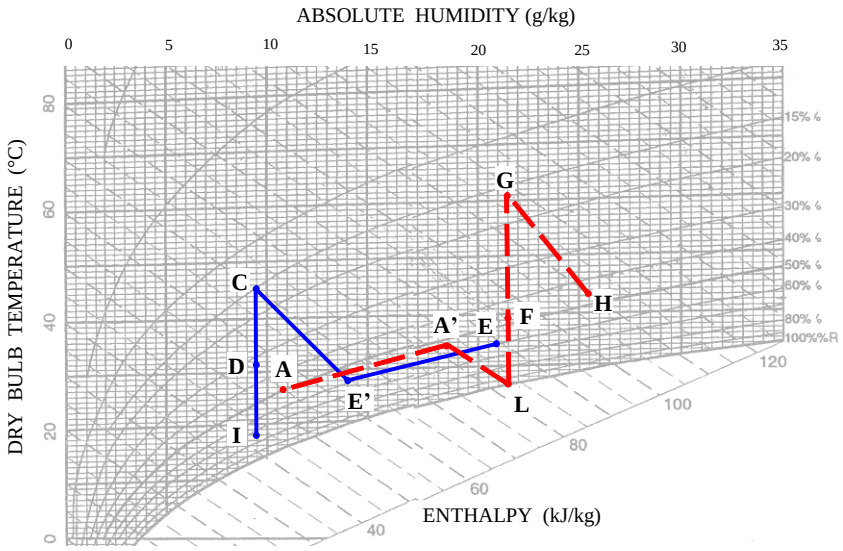

Fig. 15. Thermal cycle of the solar DEC with enthalpy wheel

The performance data of the enthalpy wheel are provided by the manufacturer and comply with the operative conditions of this case study.

This new design allows a regeneration temperature as low as T_{reg}=60°C and the elimination of the pre-cooling process.

The plot in Fig. 16, shows the improvement in all the relevant performance indexes with respect to the old design, whatever is the solar fraction. However the parameter that shows the highest increase in the comparison with the old design, is the overall exergy efficiency. It tells us that the introduction of the enthalpy wheel not only simplifies the design but also brings the benefit of primary energy savings and reduction of irreversibilities.

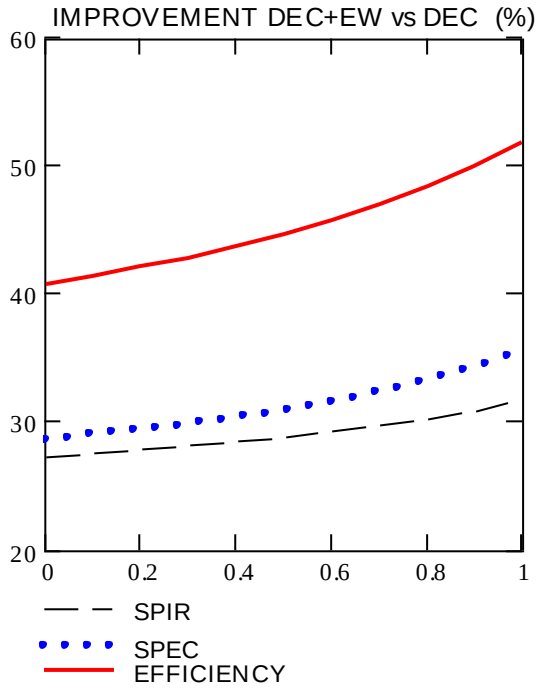

Fig. 16. Improvement of the solar DEC with enthalpy wheel to the standard solar DEC

➢ Conclusions

The exergy analysis has revealed that by lowering the regeneration temperatures not only yields less dissipative effects and improves the exergy efficiency of the AHU, but also reduces the primary energy needs.

A substantial benefit for the overall system, from both the first and second law point of view, is procured by solar energy. In a first law perspective the advantage is obviously due to the primary energy savings (only); in a second law perspective it is attributable not only to the reduced primary energy needs, but also to its relatively low energy potential, i.e. much closer than the conventional power sources to the exergy levels required by the final uses occurring in this kind of applications (heating fluids at moderate temperatures).

The final steps of this analysis have shown that these benefits can be even enhanced by the use of an enthalpy wheel, for energy recovery between supply and regeneration air.

In conclusion solar energy adds thermodynamic value to the DEC system and promotes this technology in the air conditioning market.

Finally, this study has attempted to demonstrate that a second law based analysis yields new insights on thermal processes and provides information not obtainable from a first law analysis. It is also able to steer the design towards the primary energy savings and the appropriate use of the energy sources.

REFERENCES

FUNDAMENTAL BOOKS ON EXERGY & SECOND LAW ANALYSIS

[1] Baher H.D.: Thermodynamik . Springer Verlag, 2000,

[2] Wark K. Advanced Thermodynamics for engineers, McGraw-Hill, 1995

[3] Bejan A.: Advanced Engineering Thermodynamiccs. Wiley 1988

[4] Bejan A., Tsatsaronis G., Moran M.: Thermal design and optimization, Wiley, 1996.

[5] Borel L. : Thermodynamique et energetique; Presse Politechniques Romandes , Lausanne, 1984

[6] Kotas T. :The exergy method of thermal plant analysis, Kriegen, 1995

[7] Moran M.: Availability Analysis. A guide to efficient energy use. ASME Press , 1989

[8] Moran. M. Shapiro J. : Fundamentals of Engineering Thermodynamics, Wiley, 1992

[9] Szargut J. : Exergy Method . Technical and ecological applications. WIT Press 2005

SPECIALIZED LITERATURE

[10] H-M. Henning (Ed.): "*Solar assisted Air-Conditioning in Buildings*", Springer 2004.

[11] Cammarata G., Fichera A., Forgia F., Marletta L. (1994) *:"Exergy analysis of basic processes of air conditioning systems*", Proceed. Int Conf. on HVAC in Cold climates, FINVAC 94. Finland Sept. 1994

[12] Cammarata G., Fichera A., Mammino L., Marletta L. (1997): " *Exergonomic optimization of an air conditioning system*" ASME Journal of Energy Resources Technology", March 1997

[13] Marletta L. : "*A comparison of methods to optimize air conditioning systems according to the exergonomic approach"*; ASME Journal of Energy Resources Technology", December 2001

[14] Motta M., Henning, H-M. : *A novel high efficient sorption system for air dehumidification (ECOS)*, International Sorption Heat Pump Conference, June 22 – 24, 2005; Denver, CO, USA, ISHPC – XXX – 2005

[15] Motta M., Henning, H-M. : *An Advanced Solar assisted sorption cycle for building air-conditioning: the ECOS potential and performance assessment,* Eurosun 2006.

[16] Pons M., Kodama A. Entropic Analysis of adsorption open cycles for air conditioning; International J. of Energy Research, 2000, 24, Part I. First and second Law analysis , pp-. 251-262 ; Part 2. Interpretation of experimental data , pp- 263-278.

[17] Ren Chengqin ; Li Nianping et al. : *Principles of exergy analysis in HVAC and evaluation of evaporative cooling schemes*; Building and environment , 37 (2002) pp. 1045-1055

[18] Wepfer W.J., Gaggioli R.A. , Obert E.F. : "*Proper evaluation of available energy for HVAC*", ASHRAE Trans. Vol. 85, Part 1, 1979, p.667-677.

3. Exergy analysis of a desiccant Air Handling Unit (P. Bourdoukan, M. Pons, E. Wurtz and P. Joubert)

Nomenclature

AHU air handling unit

COP coefficient of performance [-]

D_{ex} exergy destruction [W]

ex exergy flux [$W.kg^{-1}$]

h specific enthalpy [Jkg^{-1}]

m_a air mass flow rate [kgs^{-1}]

m_f heating fluid mass flow rate of the regeneration heat exchanger [$kg.s^{-1}$]

N_{ex} ratio of the exergy destruction to the total exergy input of the cycle [-]

Q heat flux [W]

T temperature [K]

w absolute humidity of moist air [$kg_{water\ vapor}.kg^{-1}_{dry\ air}$]

Greek symbol

η_{ex} exergy efficiency [-]

Subscripts

i i=1-9 relative to the position in the air handling unit

ex relative to exergy

f relative to the heating fluid of the regeneration heating exchanger

L losses

w liquid water

Superscripts

C subsystem C

DW desiccant wheel

E subsystem E

HS regeneration heat exchanger (heating system)

REV return evaporative cooler

SEV supply evaporative cooler

SR sensible heat regenerator

- Introduction

In a desiccant cooling cycle, energy input is heat that replaces mechanical work in the conventional vapor compression cycle. Being heat driven the desiccant system is a three temperature cycle e.g. the outside temperature, the conditioned space temperature and the heating source temperature. Unlike the conventional systems, a desiccant cooling system operates in an open configuration with mass transfer in addition to heat.

The subject of the present note is an exergy analysis of a desiccant evaporative cooling air handling unit (DEC) taking into account the open nature of the cycle.

First a desiccant cooling configuration is presented. Then a theoretical approach to take into account the open nature of the cycle (Pons and Kodama, 2000) is briefly explained. The energy and exergy balance of system components and of the overall system are presented. Finally measurements are used to evaluate the exergy destruction in the system.

- System description

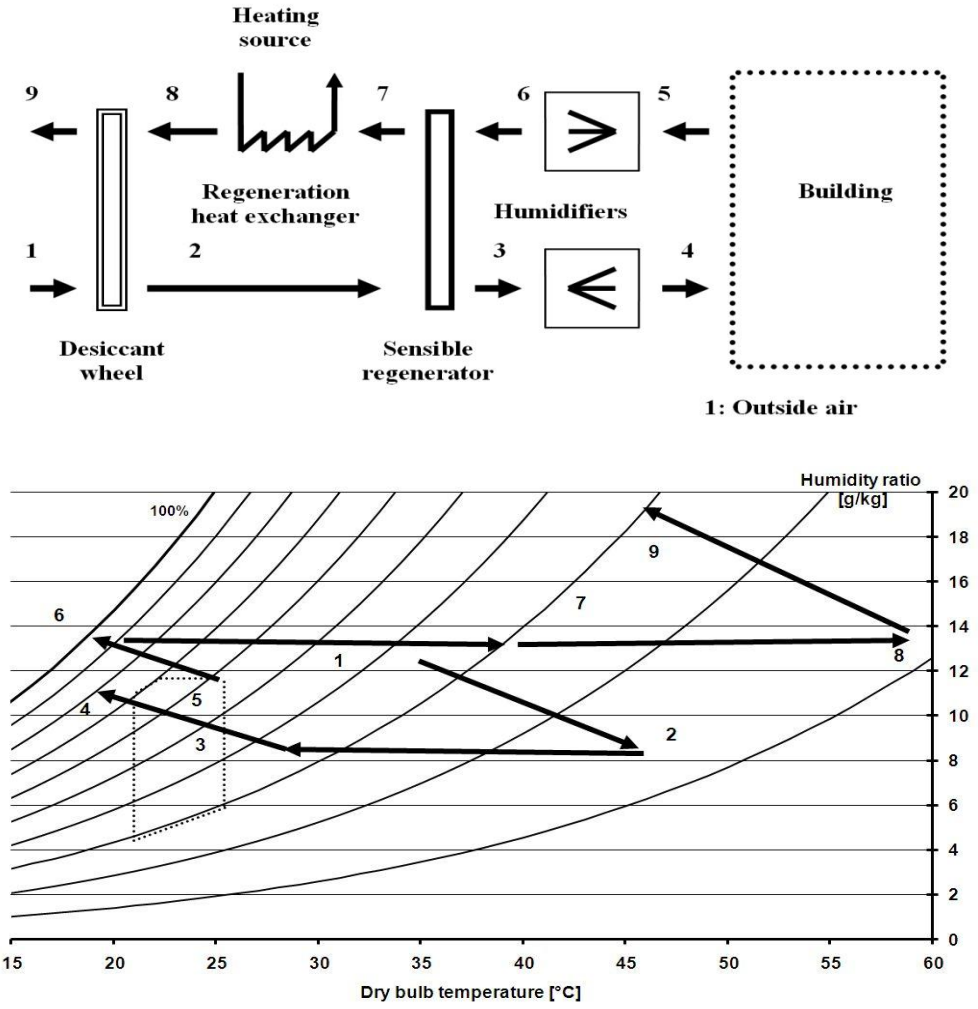

Figure 1: Desiccant cooling cycle with the corresponding evolution of air properties in the psychometric chart

In a solid desiccant cooling cycle, outside air is first dehumidified by a desiccant sorbent and then undergoes two cooling stages: first a sensible cooling stage by the return air of the building and then an evaporative cooling. With reference to figure 1 the cycle operates as follows: first, outside air (1) is dehumidified in a desiccant wheel (2); it is then cooled in the sensible rotary heat exchanger (3) by the return, cooled, air before undergoing another cooling stage by an evaporative process (4). Finally, it is introduced in the room. The operating sequence for the return air (5) is as follows: it is first cooled to its saturation temperature by evaporative cooling (6) and then it cools the fresh air in the rotary heat exchanger (7). It is then heated in the heat exchanger fed by waste heat, solar energy or a burner (8) and finally regenerates the desiccant wheel by removing the humidity before exiting the installation (9).

This cycle differs from the conventional 3 temperature cooling cycle on the following points:

A desiccant cycle exchanges heat and mass with the ambient air and with the conditioned space. Besides there is a water input to the system through the humidifiers. Pons and Kodama developed a theory to close artificially the system (Pons and Kodama, 2000) They added two theoretical subsystems C and E (Figure 2) to achieve water recycling in the system and to insure that the system exchanges only heat.

Before going into details we must pay attention to the following points:

- air state exiting the installation at position (9) is warmer and containing more water vapor than the outside ambient air (1).
- air state of the conditioned space at position (5) is warmer and containing more water vapor than the supplied air at position (4)
- at steady state, the humidity difference between the rejected air stream (9) and the ambient outside air (1) is the amount of water vapor gained through the humidifiers, and in the conditioned space.

Air exiting the installation at position (9) is mixed with outside ambient air. In this operation the air handling (AHU) unit is rejecting heat and the extra amount of humidity gained by the air flow across the AHU (through the evaporative coolers and through the conditioned space). Instead of rejecting this water gained, the purpose of subsystem C is to insure water recycling in the system and to reject only heat to the ambient atmosphere. It will remove the humidity difference between air at position 9 and air at position 1, liquefy it and send it back to the humidifiers and to the conditioned space. It also cools down air at position 9 to the temperature T_1. In this operation subsystem C rejects only heat to outside atmosphere.

Air supplied by the AHU (position 4) to the conditioned space gains heat and humidity in the space and is extracted again by the AHU (position 5). The purpose of subsystem E is heat extraction from the conditioned space thus heating up the supplied air and to insure that a part of water recycled by subsystem C is given back to the conditioned space at vapor state thus subsystem E is exchanging only heat with the conditioned space.

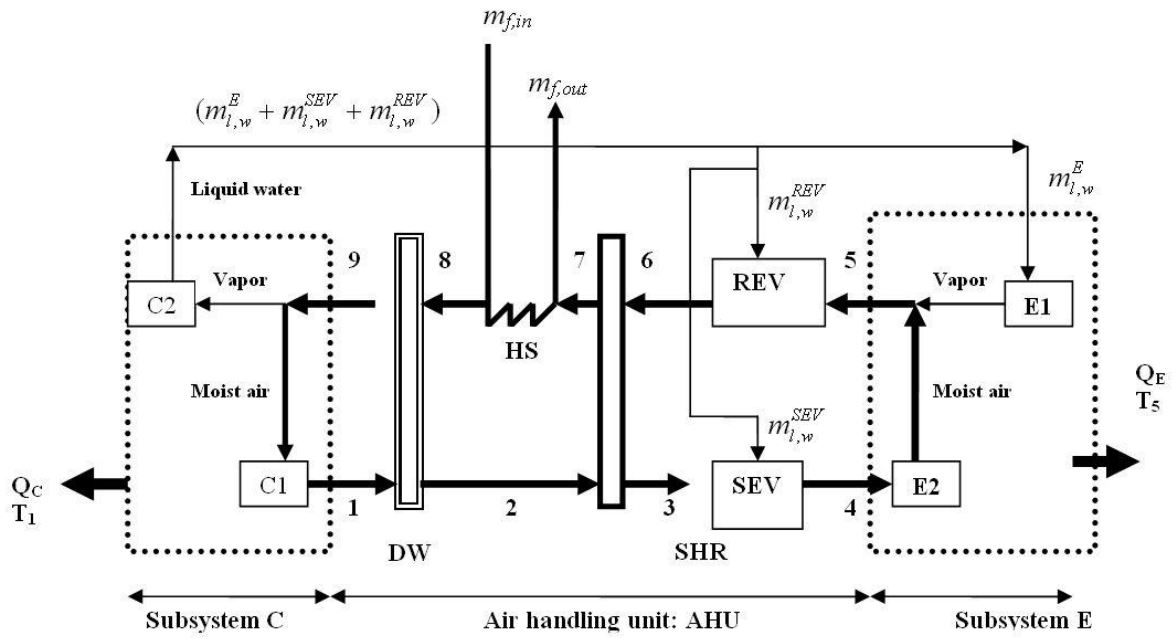

Figure 2: Introduction of subsystem C and subsystem E to close the cycle

Sub system C:

The subsystem C is composed of two ideal heat exchangers (C1 and C2) and is positioned between the exit of the air handling unit and the outside ambient air at Temperature T_1 as shown in figure 2.

Air exiting the air handling unit (state (9)) is warmer and more humid than the outside ambient air (state (1)). This air enters subsystem C and is divided into two parts the first containing all the dry air and a part of humidity which is the same humidity content of the ambient air (state (1)). This part is cooled down to T_1 using the ideal heat exchanger C1 and then becomes at the same conditions of ambient air (state (1)) and can be reintroduced in the air handling unit (AHU). The other part consists only of the excess of humidity at vapor state and is cooled down in the ideal heat exchanger C2 and then liquefied and can be delivered to the humidifiers and to the conditioned space and thus water is always re-circulated by the cycle. We must note that subsystem C rejects only heat to the outside ambient air through the heat exchangers C1 and C2.

Subsystem E:

Subsystem E is composed of two ideal heat exchangers (E1 and E2) and is positioned between the air handling unit and the conditioned space at temperature T_5.

Supply air at state (4) is fresh and less humid than the air of the conditioned space (state (5)). In the conditioned space the supply air (4) will gain heat and humidity to exit the space at state (5). To take into account this heat and humidity gain, the supply air enters the subsystem E and is first heated in the ideal heat exchanger E1 (heat is coming from the conditioned space) while a part of the water coming from subsystem C is first cooled down to T5 and evaporates at this temperature using another ideal heat exchanger E2 (only heat is exchange with the conditioned space) and then is added to the air stream and finally reintroduced into the air handling unit at state (5). In this way subsystem E exchanges only heat with the conditioned space.

The residual amount of water coming from subsystem C is supplied to the humidifiers and thus the cycle is thermodynamically closed, thanks to recycling air and water and exchanging only heat with the outside air and with the conditioned space (figure 2).

In the following section the energy, exergy and mass balances of the components and of the subsystems will be given.

- Energy and exergy balance of the desiccant Air Handling Unit under steady state conditions

Energy and exergy balances in this section does note take into account the mechanical input of the fans

Dead state:

The dead state considered is outside ambient air with temperature T_1 and humidity ratio w_1.

Energy and exergy balance of the desiccant wheel:

$$m_a(h_1 - h_2) + m_a(h_8 - h_9) - Q_L^{DW} = 0 \quad (1)$$

$$m_a(ex_1 - ex_2) + m_a(ex_8 - ex_9) - D_{ex}^{DW} = 0 \quad (2)$$

Energy and exergy balance of the sensible heat regenerator

$$m_a(h_2 - h_3) + m_a(h_6 - h_7) - Q_L^{SR} = 0 \quad (3)$$

$$m_a(ex_2 - ex_3) + m_a(ex_6 - ex_7) - D_{ex}^{SR} = 0 \quad (4)$$

Energy, exergy and mass balance of the supply evaporator cooler SEV

$$m_a(h_3 - h_4) + m_w^{SEV} h_w - Q_L^{SEV} = 0 \quad (5)$$

$$m_a(ex_3 - ex_4) + m_w^{SEV} ex_w - D_{ex}^{SEV} = 0 \quad (6)$$

$$m_a(w_3 - w_4) + m_w^{SEV} = 0 \quad (7)$$

Energy, exergy and mass balance of the return evaporator cooler REV:

$$m_a(h_5 - h_6) + m_w^{REV} h_w - Q_L^{REV} = 0 \quad (8)$$

$$m_a(ex_5 - ex_6) + m_w^{REV} ex_w - D_{ex}^{REV} = 0 \quad (9)$$

$$m_a(w_5 - w_6) + m_w^{REV} = 0 \quad (10)$$

Energy and exergy balance of the regeneration heat exchanger HS:

$$m_a(h_7 - h_8) + m_f(h_{f,in} - h_{f,out}) - Q_L^{HS} = 0 \quad (11)$$

$$m_a(ex_7 - ex_8) + m_f(ex_{f,in} - ex_{f,out}) - D_{ex}^{HS} = 0 \quad (12)$$

Energy, exergy and mass balance of the subsystem C:

$$m_a(h_9 - h_1) - (m_w^{SEV} + m_w^{REV} + m_w^E)h_w - Q^C = 0 \quad (13)$$

$$m(ex_9 - ex_1) - (m_w^{SEV} + m_w^{REV} + m_w^E)ex_w - D_{ex}^C = 0 \quad (14)$$

$$m_a(w_9 - w_1) - (m_w^{SEV} + m_w^{REV} + m_w^E) = 0 \quad (15)$$

Energy , exergy and mass balance of the subsystem E:

$$m_a(h_4 - h_5) + Q^E + m_w^E h_w = 0 \quad (16)$$

$$m_a(ex_4 - ex_5) + m_w^E ex_w + Q_E(1 - \frac{T_1}{T_5}) + D_{ex}^E = 0 \quad (17)$$

$$m_a(w_5 - w_4) - m_w^E = 0 \quad (18)$$

Energy and exergy analysis of the air handling unit

$$m_a(h_1 - h_9) + m_a(h_5 - h_4) + (m_w^{SEV} + m_w^{REV})h_w + m_f(h_{f,in} - h_{f,out}) - Q_L^{AHU} = 0 \quad (19)$$

$$m_a(ex_1 - ex_9) + m_a(ex_5 - ex_4) + (m_w^{SEV} + m_w^{REV})ex_w + m_f(ex_{f,in} - ex_{f,out}) - D_b^{AHU} = 0 \quad (20)$$

Where

$$Q_L^{AHU} = Q_L^{DW} + Q_L^{SR} + Q_L^{HS} + Q_L^{SEV} + Q_L^{REV} \quad (21)$$

$$D_{ex}^{AHU} = D_{ex}^{DW} + D_{ex}^{SR} + D_{ex}^{HS} + D_{ex}^{SEV} + D_{ex}^{REV} \quad (22)$$

The COP of the air handling unit

$$COP = \frac{Q_E}{m_f(h_{f,in} - h_{f,out})} \quad (23)$$

The exergy efficiency of the cycle is then:

$$\eta_{ex} = \frac{-Q_E(1 - \frac{T_1}{T_5})}{m_f(ex_{f,in} - ex_{f,out})} = 1 - \frac{D_{ex}^{AHU} + D_{ex}^C + D_{ex}^E}{m_f(ex_{f,in} - ex_{f,out})} = 1 - \frac{D_{ex}^{DW} + D_{ex}^{SR} + D_{ex}^{HS} + D_{ex}^{SEV} + D_{ex}^{REV} + D_{ex}^E + D_{ex}^C}{m_f(ex_{f,in} - ex_{f,out})}$$

(24)

Introducing the variable N_{ex}^{x} as the ratio of the exergy destruction D_{ex}^{x} of component x over the exergy input of the cycle $m_f(ex_{f,in} - ex_{f,out})$, the exergy efficiency can be thus written as:

$$\eta_{ex} = 1 - N_{ex}^{DW} + N_{ex}^{SR} + N_{ex}^{HS} + N_{ex}^{SEV} + N_{ex}^{REV} + N_{ex}^{E} + N_{ex}^{C} \quad (25)$$

- Brief description of the experimental setup

Figure 3 shows the experimental setup (Bourdoukan, 2008), (Bourdoukan et al, 2008) used to investigate the desiccant cooling technology. The air handling unit consists of a desiccant wheel, a sensible heat regenerator, two humidifiers and a regeneration heat exchanger (water to air).

- The desiccant wheel is a honeycomb structure using silica gel as a desiccant with the angular velocity of 8 rev.h^{-1} for a nominal air flow rate of 3000 m^3.h^{-1}.
- The sensible heat regenerator is an aluminum honeycomb structure. It rotates at 12 rev.min^{-1}.
- The system is provided with motor driven rotating centrifugal humidifiers
- The regeneration heat exchanger is a conventional cross flow heating coil, widely used in air handling units.
- The air handling unit is powered by 40 m^2 of heat-pipe vacuum-tube collectors feeding a storage tank of 2,350 liters.

- Measurements:

Special attention was paid to the accuracy of the measurements.

Psychrometers were used to measure the moist air properties (temperature and humidity) in the air handling unit. Each psychrometer consists of two Pt100 sensors: the first delivers the dry bulb temperature while the second - covered by a wick constantly soaked in distilled water - gives the wet bulb temperature. Since the local atmospheric pressure is measured, the humidity ratio and relative humidity are thus accurately measured.

Temperature in the hydraulic loop is measured by means of Pt100 sensors integrated to the pipes by means of thermo wells. All the Pt100 sensors (psychrometers and hydraulic loop) were tuned on a temperature range of 0°C to 100°C.

Ultrasonic sensors were used to measure the water flow rates in the hydraulic loop while gas tracer method was used for the airflow rate measurement.

All the sensors were connected to a central computer via an acquisition unit and thus 3 graphical interfaces were developed: the first for the air handling unit, the second for the solar installation and the third for outside conditions.

For the uncertainty of the measurements please check (Bourdoukan et al, 2009).

Figure 3: Experimental installation with the solar collector field

- Results

Operative conditions

Air flow rate m_a 1 $kg.s^{-1}$
Water flow rate m_f of the regeneration heat exchanger 1 $kg.s^{-1}$
Outside temperature: T_1 28°C
Outside humidity ratio w_1 13.3 $g.kg^{-1}$
Fluid temperature inlet of the regeneration heat exchanger 63.5°C
Fluid temperature outlet of the regeneration heat exchanger 57.8°C
Regeneration temperature T_8 60°C
Return temperature T_5 26°C
Return humidity ratio w_5 11.1 $g.kg^{-1}$

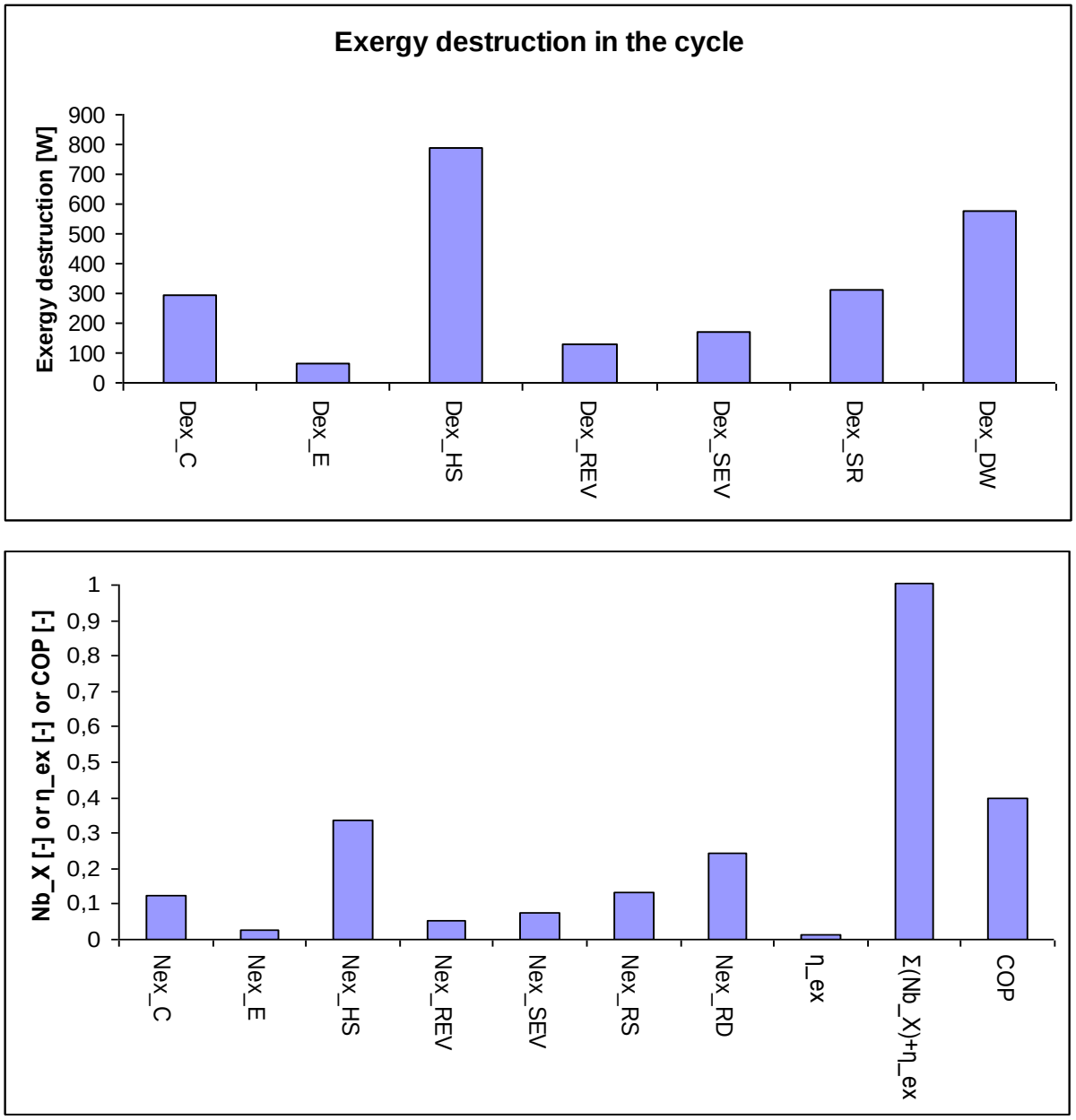

Figure 4: Exergy calculation results: Top: Exergy destruction in components, bottom exergy ratio of components, exergy efficiency of the cycle and the COP

- Results of exergy analysis , based on experimental data

The exergy analysis of the whole system was conducted on the basis of the experimental data, given above. The results can be summarized as follows.

Figure 4 shows the exergy destruction in each component of the air handling unit as well as the exergy destruction in the subsystems C and E. In the histogram at the top exergy destructions (irreversibilities) in the components are shown in absolute values while in the bottom histogram they are shown with respect to the exergy input of the cycle.

The last three bars show respectively

- the exergy efficiency of the cycle
- the consistency of the calculation method since $\eta_{ex} + \sum(N_b^x)$ must be equal to unity
- the COP

The exergy efficiency of the air handling unit is 0.131. This low value of the exergy efficiency is due to various irreversibilities that occur in the components, besides that irreversibility due to the open nature of the system (i.e subsystem E and C).

The results show that exergy destruction occurs on a high level in the regeneration heat exchanger (33.7%) and in the in the desiccant wheel (24.5%)

On a second level comes exergy destruction in the sensible heat regenerator (13.3%) and in the subsystem C (12.5%).

On a less important level exergy is destructed in the evaporative coolers (7.35% and 5.45%) and in subsystem E (2.6%).

- Comments

Desiccant wheel: Irreversibilites in the desiccant wheel are of two different types: those of heat transfer across finite temperature difference and mass transfer across finite partial pressure difference (Van den Bulck and Mitchell, 1988) and those due to the mixing at the outlet of the desiccant wheel of air streams with different temperature and humidity ratio. In fact at the outlet of the desiccant wheel, air is not homogeneous with a significant temperature and humidity ratio difference due to the low rotation speed of the wheel. The mixing of these air streams to give uniform conditions at the outlet of the desiccant wheel, is irreversible.

A part of exergy destruction can be avoided by a non rotating matrix that reduces the non homogeneous profile at the outlet of the desiccant wheel.

Regeneration heat exchanger: In the heating system exergy destruction is produced by heat transfer across finite temperature difference. With this configuration this contribution to the irreversibilities depends mostly on the temperature required by the regeneration process.

Sensible heat regenerator: In the sensible regenerator, exergy destruction is due to the heat transfer across finite temperature difference and to the mixing of inhomogeneous air streams at the outlets of the sensible regenerator. Here the temperature difference between air streams at the outlet is lower than for the desiccant wheel; moreover, in the case of the sensible regenerator, the humidity ratio of the two air streams is constant.

An improvement of the exergy performance of the sensible regenerator can be achieved by using a non rotating matrix (attention must be paid to the thermal efficiency of the heat exchanger that must be high otherwise the COP drops significantly)

Evaporative coolers: In these devices irreversibilities are due to three different mechanisms. The first is heating or cooling the supply water by the air to the temperature of the air. The second is the evaporation of the water and the third is the mixing of the water vapor with moist air. The calculations of the three steps showed that most of the irreversibilities occur in the mixing stage, since heating and evaporating water are reversible processes. Although

small, this part can not be avoided since the cooling provided by the system is by evaporative process.

Subsystem C: The main source of irreversibility in subsystem C is the split operation that occurs before C1 and C2. This split operation is a representation of the fact that the air is exiting the installation (position 9) at higher temperature and humidity ratio than the outside air (position 1). This mixing process of the ejected air with outside air is irreversible.

Subsystem E: As in subsystem C the main source of irreversibility in the subsystem E is the mixing that occurs in the ideal heat exchangers E1 and E2. This represents the irreversibility that occurs when the supply air (position 4) at low temperature and humidity ratio meets with the conditioned space (position 5) taken at higher temperature and humidity ratio. This part is much lower than in subsystem C since the supply condition especially humidity w_4 differs a little than the return humidity w_5. While in subsystem exit conditions (T_9 and w_9) are much higher than (T_1, w_1) and the irreversibility produced by mixing is then higher.

This shows that the open nature of cycle has a non negligible part of irreversibility of the process (15%) and is intrinsic to the system.

- Conclusions

The exergy analysis conducted above has shown that, as far as the Air Handling Unit of a DEC is concerned, possible improvements can be achieved by using fixed bed heat exchangers and desiccant wheels instead of rotating devices and by adopting desiccant materials less demanding in terms of regeneration temperature. Although not considered here, also parasitic losses and electric consumption to drive pumps, fans, motors and control devices should obviously be taken as low as possible.

REFERENCES

Pons, M., and Kodama, A. (2000). "Entropic analysis of adsorption open cycles for air conditionning. Part1: first and second law analyses." *International Journal of Energy Research*, 24, 251-262.

Bourdoukan, P., (2008). "Etude numérique et expérimentale destine à l'exploitation des techniques de rafraîchissement par dessiccation avec régénération par énergie solaire" *PhD Thesis*, Université La Rochelle, La Rochelle.

Bourdoukan, P., Wurtz, E. and Joubert, P. (2009) "Experimental investigation of a solar desiccant cooling installation" *Solar Energy*, 83 (2009) 2059-2073.

Van den Bulck, E., S.A, K., and Mitchell, J. W. (1988). "Second law analysis of solid desiccant rotary dehumidfiers." *Journal of Solar Energy Engineering*, 110, 2-9.

4. Exergy analysis of an Evaporatively COoled Sorptive Heat Exchanger (Constanze Bongs)

➢ System description

A new development of a system concept called ECOS (Evaporatively cooled sorptive heat exchanger) for small air-flow capacities up to 400 m³/h is currently under development at Fraunhofer ISE.

The ECOS system concept consists of two air-to-air plate heat exchangers which unite air dehumidification by adsorption and air cooling by indirect evaporative cooling in a single component.

The plate heat exchanger is divided into desiccant-coated sorptive channels and cooling channels which are in thermal contact. Ambient air passing the sorptive channels is dehumidified and simultaneously cooled by indirect evaporative cooling. Indirect evaporative cooling is achieved through evaporation of water sprayed into the cooling channels.

Therefore, the heat of adsorption is removed. This leads to the cooling of the sorptive matrix and to an enhanced sorption capacity in comparison to adiabatic processes such as in a dehumidifier wheel. In order to provide a continuous supply air flow to the building, the two heat exchangers are operated alternately – while one heat exchanger is in adsorption mode providing air dehumidification and cooling, the second heat exchanger is regenerated and pre-cooled (Fig 1).

The main advantages of the ECOS cooled sorptive heat-exchanger concept are the enhanced dehumidification, the simultaneous air cooling and dehumidification and the strict separation of the supply and the return air flow, avoiding carry-over effects common in rotary DEC systems.

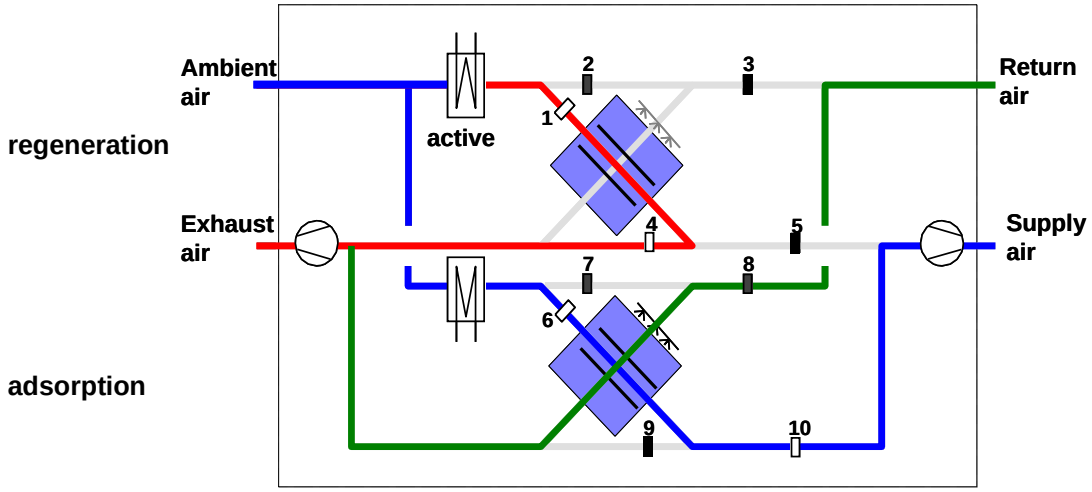

Fig 1: ECOS system concept: regeneration of the upper heat exchanger and ambient air dehumidification and cooling in the lower heat exchanger

➢ Operating Behaviour

Aimed at the performance prediction, a model of the sorptive heat exchanger was implemented using the object-oriented modelling language Modelica [12]. In the course of a

collaborative research project a prototype of a sorptive heat exchanger is also being built, while model validation is currently ongoing. Modelling results are used as data base for the exergy analysis, instead of measured data, to avoid a distortion of the analysis due to measurement uncertainty.

A module of a sorptive coated heat exchanger has been implemented for the analysis. The simulated counter flow heat exchanger is characterized by a volume flow rate of 20 m^3/h per square meter of heat transfer area (effective heat transfer area of 20 m^2). It is covered by a silicagel layer (Grace 127B) and discretized in ten elements in flow direction. Table 1 gives the state of air properties as applied in the baseline simulation.

Table 1: Input air properties during different cycle stages as used in the simulation

Air flow properties: Sorption channel inlet				Air flow properties: Cooling channel inlet			
$\dot{m}_{ads}$	Ambient air	$\dot{m}_{des}$	Heated ambient air	$\dot{m}_{ads}$	Building return air	$\dot{m}_{pre-cool}$	Ambient air
T_{ads} [°C]	32.0	T_{des}	85.0	T_{ads}	26.0	$T_{pre-cool}$	32.0
ω_{ads} [g/kg]	14.7	ω_{des}	14.7	ω_{ads}	12.5	$\omega_{pre-cool}$	14.7
φ_{ads} [%]	50.0	φ_{des}	4.1	φ_{ads}	60.0	φ_{des}	50.0

The sequence of different cycle stages characteristic for the process can be described with the help of Fig 2. It shows the air streams flowing through the sorption and cooling channels during these different cycles stages.

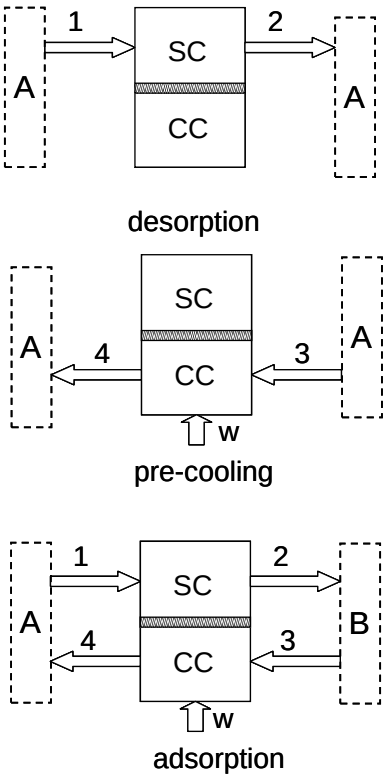

Fig 2: Flow streams corresponding to different cycle stages of the ECOS heat exchanger (where SC: sorptive channel, CC: cooling channel, w: water, A: ambient, B: building)

During desorption, the ambient air (A), heated by an external source up to the regeneration temperature (typically between 60 to 85 °C), flows through the sorption channels. The water adsorbed at the surface of the desiccant material is desorbed by the hot regeneration air. During this process the water changes from the bound liquid to the vapour phase. The water vapour, entrained by the air stream, is expelled to the ambient (A). At the end of the desorption stage, the heat exchanger is regenerated but hot.

The aim of the subsequent pre-cooling stage is to cool down the heat exchanger. To this purpose, ambient air is evaporatively cooled before and in the cooling channels by spraying water onto the heat exchanger.

In the third stage - adsorption - which represents the main operation of the sorptive heat exchanger, ambient air is flowing through the sorption channels where it is dehumidified and cooled and then supplied to the building (B). Building return air is evaporatively cooled in the cooling channels of the heat exchanger and then expelled to the ambient (A) as exhaust air.

In the following, the simulation results applied in the subsequent analysis are presented. Fig 3 shows the outlet and inlet temperature of the process air flow, while Fig 4 gives the humidity ratio for the sorptive heat exchanger. Both figures refer to one entire cycle comprising desorption, pre-cooling and adsorption (dehumidification).

The first cycle stage depicted in Fig 3 and Fig 4 is desorption when hot ambient air flows through the process air channels for regeneration. Temperature T_2 first rises sharply due to the heating up of the heat exchanger. Concurrently, outlet humidity ratio ω_2 also rises sharply due to the high driving potential for desorption caused by the rising water load and temperature of the desiccant material. As desorption proceeds and the desiccant material is getting dryer, the driving potential and consequently the outlet humidity ratio ω_2 diminishes. At the same time the outlet temperature T_2 rises.

During the pre-cooling stage, the ambient air flows through the cooling channels where it is humidified. Fig 3 shows how the outlet temperature T_4 of air leaving the cooling channels decreases as the heat exchanger cools down. It reaches a temperature below ambient temperature (T_3) due to the evaporative cooling. During pre-cooling, sorption channel air properties are not shown due to zero air flow rate.

During adsorption ambient air flows through the sorption channels and building exhaust air passes the cooling channels being simultaneously humidified. As given in Fig 4 dehumidification is most effective at the beginning of the adsorption phase (ω_2 rises sharply) as the sorption material water load is still low. The process air outlet temperature T_2 results lower at the end of the adsorption stage, as less heat of adsorption is released with decreasing dehumidification. In the counter flow arrangement simulated here, the exhaust air temperature T_4 at the cooling channel outlet is higher than the process air outlet temperature T_2.

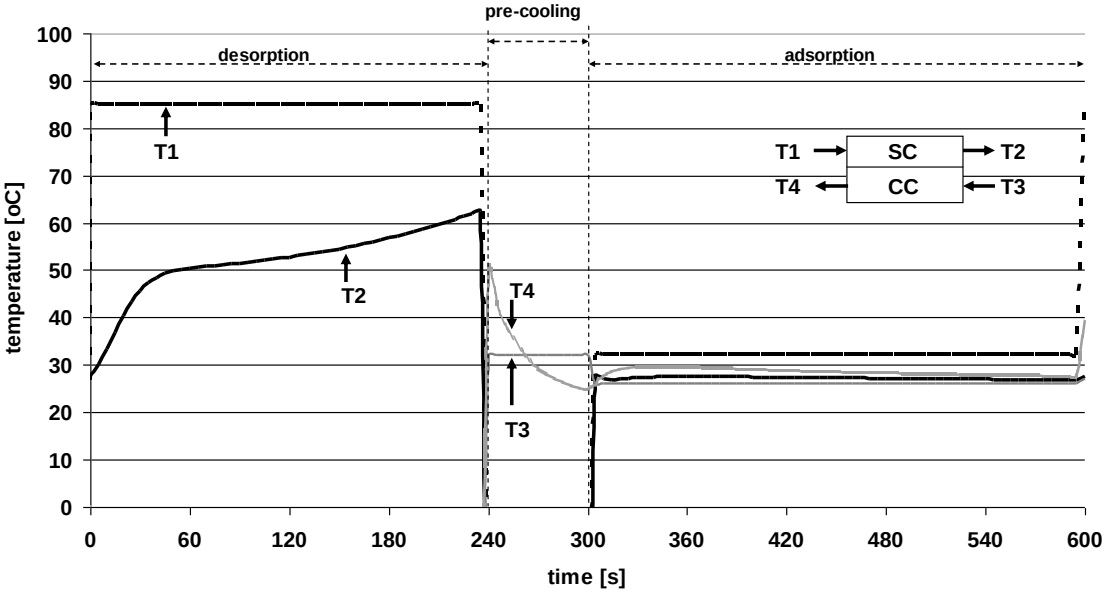

Fig 3: Temperature distribution of outlet and inlet air during one cycle

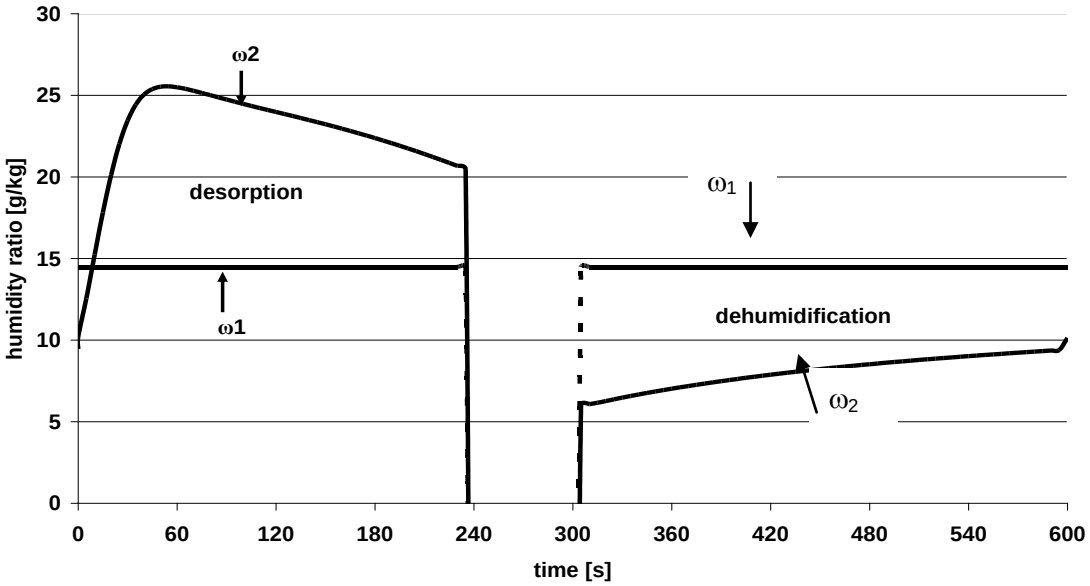

Fig 4: Humidity distribution of outlet process air during one cycle

Methodology of exergy analysis of the ECOS process

- Exergy definition and exergy reference definition

The application of the exergy method to moist air processes such as air-conditioning, drying and wet cooling tower processes was first described by Szargut [4]. A pathbreaking publication for the application in HVAC was later written by Wepfer [5]. Processes of evaporative cooling [6,7] and rotary type desiccant systems [8,9] were later both covered.

Equation 1 is the generally applied moist air specific exergy equation written on a per mass of dry air basis [4,5]: [J/kg]

$$e_a = (c_{p,da} + \omega \cdot c_{p,v})\left(T - T_0 - T_0 \ln \frac{T}{T_0} \right) + (1+\tilde{\omega}) R_a T_0 \ln \frac{p}{p_0} + R_a T_0 \left[(1+\tilde{\omega}) \ln \frac{(1+\tilde{\omega}_0)}{(1+\tilde{\omega})} + \tilde{\omega} \ln \frac{\tilde{\omega}}{\tilde{\omega}_0} \right] \quad (1)$$

with $\tilde{\omega} = \frac{M_a}{M_w} \omega \approx 1.608\omega$ [mol/mol] (2)

where the three summands represent the thermal, mechanical and chemical exergy of moist air.

An important issue for the application of exergy to moist air is the selection of the dead state. In the literature, both selecting either ambient conditions or saturated air at ambient temperature is discussed. The latter approach discussed by Chengqin [7] was followed in a conference paper [11]. In order to obtain results comparable to the other contributions within the Task 38 working group on exergy analysis, ambient temperature and humidity ratio are here used as the reference state.

The exergy of water used for evaporation is generally described by equation 3 and is derived from analyzing a process where water is condensed from ambient air [5]:

$$e_w = h(T) - h(T_0) - T_0 \left[s(T) - s(T_0) \right] + \left[p - p_{sat}(T) \right] v_w(T) - R_v T_0 \ln \phi_0 \quad \text{[J/kg]} \quad (3)$$

When choosing ambient air temperature and humidity ratio as reference conditions, the last term is dominating.

- Exergy analysis of the ECOS system

Exergy analysis is either applied for the identification of system irreversibilities via the calculation of exergy losses and exergy destruction, or for the assessment of system performance by calculating the exergy efficiency. As the system under consideration is characterized by cyclic operation (Fig 1 and Fig 2), two approaches to exergy analysis are imaginable. Firstly, each cycle stage could be subject to an exergy analysis which would require taking into account the exergy of the sorption material and the adsorbate.

Secondly, it is possible to look at the entire cycle characterized by equal sorption material load and temperature at the beginning and end of the cycle. This second approach is followed here and allows setting the system boundary as given in Fig 5. Therein, the sorption material is completely included, thus it is not separately appearing in the exergy balance.

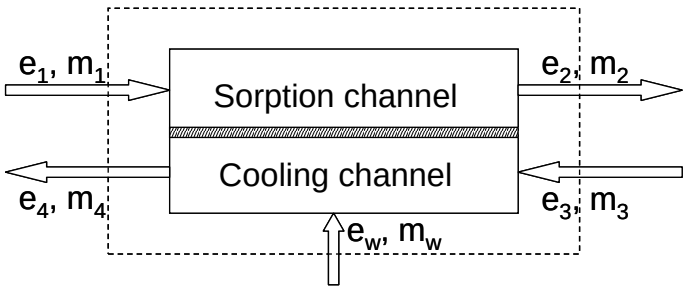

Fig. 5: System boundaries definition

When dealing with cyclic operation, it is suitable to state the exergy balance in terms of cumulated exergy for each flow stream per cycle stage, such as:

$$E_i = \int_{t=start}^{t=end} \dot{m}_i e_i dt$$

with $E_w=E_3=E_4=0$ during the desorption stage and $E_1=E_2=0$ during the pre-cooling stage due to zero mass flow rate. The overall exergy balance for the cycle can then be expressed by the following equation:

$$\sum\left(E_1 + E_3 + E_w\right) - \sum\left(E_2 + E_4\right) = E_D$$

The average exergy destruction rate of a single heat exchanger can be obtained dividing by the cycle time. The exergy efficiency can be expressed as ratio of the net useful output (product) to the net input exergy:

$$\eta_{ex} = \frac{E_{2,ads} - E_{1,ads}}{\sum\ (E_3 - E_4 + E_w)}$$

ECOS heat exchanger exergy analysis

In this study the performance of the ECOS heat exchanger is given in terms of exergy destruction (irreversibility) and exergy efficiency. A parametric analysis was carried out with respect to a variation in regeneration temperature. Further, an improved system configuration of the ECOS system will be discussed.

The results presented here are obtained by applying constant ambient conditions as exergy reference conditions (T_{ref}= 32 °C and ω_{ref} =14.7 g/kg). Choosing constant reference conditions allows a comparison of varying operating parameters and system configurations. As the exergy efficiency is highly dependent on the reference state, the exergy efficiencies given here may however not be applied for the comparison with other analyses (and systems) in which a different reference state is chosen.

- Role of the Regeneration Temperature

Figure 6 shows that a rising regeneration temperature causes a sharp increase in exergy destruction and a drop in the exergetic efficiency. This behaviour of the ECOS system, which is in common with the rotary type DEC systems, can be explained with the fact that the higher the regeneration temperature, the higher are the irreversibilities in the heat transfer process. Moreover, significant exergy losses occur in the desorption stage, due to the release to the ambient of the regeneration air, at a temperature relatively higher than ambient.

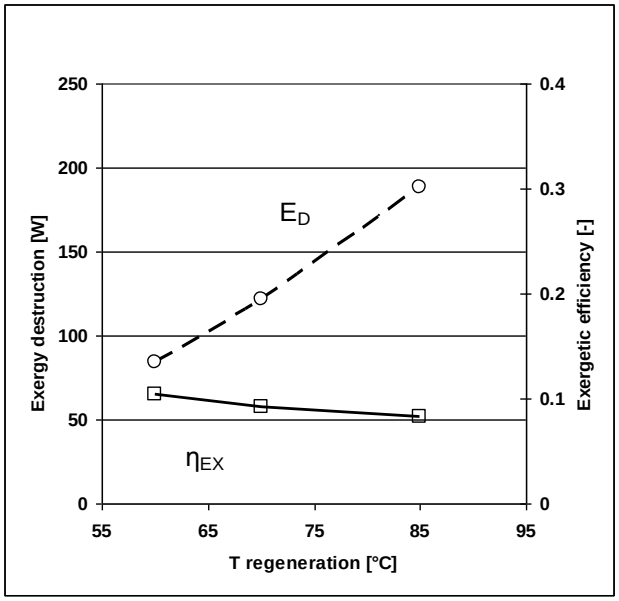

Fig 6: Exergetic performance dependent on regeneration temperature. Inlet conditions as in Table 1

- Improved system configuration

An improved system configuration would maximize the exergy product and minimize the exergy input, increasing the exergetic efficiency. Maximizing the exergetic product could theoretically be realized during adsorption by further cooling the dehumidified process air by an additional indirect evaporative cooler (Fig 7). A minimization of the exergetic input could be achieved during desorption by exploiting the exergy of the air leaving the sorptive heat exchanger for the pre-heating of the regeneration air (Fig 8). This simultaneously implies a reduction of exergy losses.

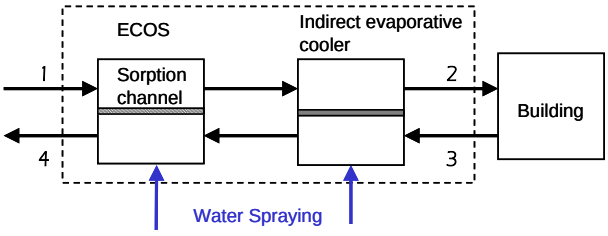

Fig 7: Increase of exergetic product in the adsorption stage: further decrease of the supply air temperature by an additional indirect evaporative cooler

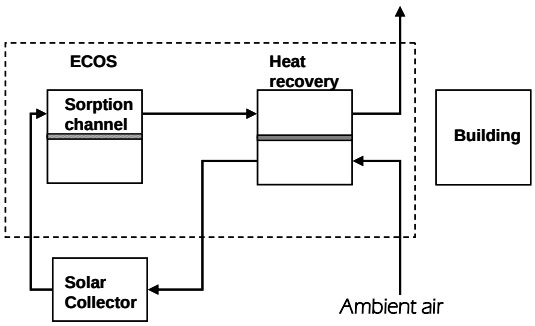

Fig 8: Simultaneous reduction of exergy losses and exergetic input in the desorption stage: heat recovery to pre-heat regeneration air

Simulations were performed for an enhanced system configuration including both measures of improvement. The heat exchanger for heat recovery was characterized by an efficiency of 80% and simulations were performed for a regeneration temperature of T_{reg}=60°C. All the remaining inlet conditions are equivalent to the previous analysis and can be found in Table 1. The following Table 2 gives the averaged outlet conditions of the adsorption stage for the basic and the improved system configuration (operation as in Fig 7).

Table 2: Averaged air properties during adsorption for the basic and the improved system configuration (regeneration temperature of 60°C)

	1: Ambient air	2: Supply air	3: Return air	4: Exhaust air
Basic configuration	T = 32.0 °C ω = 14.7 g/kg	T = 26.0 °C ω = 10.0 g/kg	T = 26.0 °C ω = 12.5 g/kg	T = 27.4 °C ω = 19.4 g/kg
Improved configuration	T = 32.0 °C ω = 14.7 g/kg	T = 22.4 °C ω = 10.0 g/kg	T = 26.0 °C ω = 12.5 g/kg	T = 28.0 °C ω = 20.7 g/kg

The additional evaporative cooler (Fig 7) leads to a lower supply air temperature T_2 to the building. Therefore, the useful effect of the system is enhanced – the exergetic product can be increased by 58%. To further increase the exergetic efficiency, the exergy input should be minimized.

Looking at the exergy input to the enhanced system configuration, two effects must be analyzed. Due to the heat recovery, the exergy input for the regeneration decreases by 15%.

Moreover, the additional indirect evaporative cooling requires a higher amount of water. When using (non-saturated) ambient humidity as reference state, the exergy attributed to the liquid water implies a rise of the exergy input by 2%, which partially counterbalances the exergy input savings due to the heat recovery. However, the overall exergetic efficiency of the improved system rises from 0.10 to 0.15. Also the thermal COP, defined as the ratio of removed heat to the heat input during desorption, increases from 0.75 for the basic to 1.01 for the improved configuration.

➢ Conclusions

Simulation results of a dynamic model of a sorptive heat exchanger were presented in an exergetic framework. The reference state of the second law analysis was set constant and at ambient conditions in order to allow comparability of the results of the different analyses conducted in this contribution. T

The second law analysis showed how to enhance system efficiency with respect to 1. the operating parameter regeneration temperature and 2. with respect to an improved system configuration.

Decreasing the regeneration temperature leads to a decrease in irreversibility of the heat exchange process, leading to a higher exergy efficiency. The improved system configuration included 1. an additional indirect evaporative cooler in the adsorption stage and 2. a recuperator for pre-heating the regeneration air flow in the desorption stage. This combination of improvements leads to an increase of the exergy product and a decrease of the exergy input. Therefore, the overall exergy efficiency rises by 50% and the thermal COP by 35 %, with respect to the basic design.

These findings apply to the system's thermal behaviour. Including the consideration of parasitic losses (fan power), which are highly dependent on the actual system layout, should be subject of future work.

Nomenclature and Subscripts

Nomenclature				**Subscripts**			
c	specific heat capacity [J/kgK]	M	molar mass [g/mol]	a	air	v	vapour
E	exergy [J]	m	mass [kg]	D	destruction	w	water
e	specific exergy [J/mol, J/kg]	v	specific volume [m^3/kg]	da	dry air	0	reference state
p	pressure [Pa]	η	efficiency [1/100]	ex	exergetic	1…4	state points
R	specific gas constant [J/molK]	φ	relative humidity [%]	p	constant pressure		
T	temperature [K, °C]	ω	humidity ratio [kg/kg]	sat	saturation		

REFERENCES

[1] Motta, M., Henning, H.-M. (2005): A novel high efficient sorption system for air dehumidification (ECOS), International Sorption Heat Pump Conference, June 22-24, Denver, CO, USA.

[2] Schicktanz, M., Nunez, T. (2008): Modelling af an adsorption chiller for dynamic system simulation, International Sorption Heat Pump Conference, Seoul, Korea, September 2008, in press.

[3] Bosnjakovic, F. (1997): Technische Thermodynamik, Teil II, 6. Auflage, Steinkopf, Darmstadt.

[4] Szargut, J., Stryrylska, T. (1969): Die exergetische Analyse von Prozessen der feuchten Luft, Heizung, Lueftung, Haustechnik, 5, 173-178.

[5] Wepfer, W.J., Gaggioli, R.A., Obert, E.F.(1979): Proper evaluation of available energy for HVAC, ASHRAE Transactions, 667-677.

[6] Taufiq, B., Masjuki, H., Mahlia, T., Amalina, M., Faizul, M., Saidur, R. (2007): Exergy analysis of evaporative cooling for reducing energy use in a Malaysian building. Desalination, 209, 238-243.

[7] Chengqin, R., Ninping, L. Guanga, T. (2002): Principles of exergy analysis in HVAC and evaluation of evaporative cooling schemes. Building and Environment, 37, 1045-1055.

[8] Taufiq, B., Masjuki, H., Mahlia, T., Amalina, M., Faizul, M., Saidur, R. (2007): Exergy analysis of evaporative cooling for reducing energy use in a Malaysian building. Desalination, 209, 238-243.

[9] Kanoglu, M., Carpinlioglu, M., Yildirim, M. (2004): Energy and exergy analyses of an experimental open-cycle desiccant cooling system. Applied Thermal Engineering, 24, 919-932.

[10] Camargo, J., Ebinuma, C., Silveira, J. (2003): Thermoeconomic analysis of an evaporative desiccant air conditioning system. Applied Thermal Engineering, 23, 1537-1549.

[11] Bongs, C., Henning, H.-M., Morgenstern, A. (2008): Modelling and exergetic assessment of a sorptive heat exchanger for the application in a novel desiccant evaporative cooling cycle. Proc. EuroSun 2008, Lisbon, October 7-10, Portugal.

[12] Bongs, C., Morgenstern, A., Henning, H.-M. (2009): Evaluation of Sorption Materials for the Application in an Evaporatively Cooled Sorptive Heat Exchanger, Proc. HPC2009, Berlin, September 7-9, Germany.

5. THERMODYNAMIC COMPARISON OF DIFFERENT DESIGNS OF SINGLE STAGE AMMONIA / WATER ABSORPTION HEAT PUMPS
(Harald Moser & René Rieberer)

➢ Introduction

In this chapter two thermodynamic models are described in order to compare two designs of an ammonia/water absorption heat pump and to calculate the thermodynamic penalty of a co-current flow in the generator compared to a counter-current flow. Therefore an exergy analysis has been carried out to identify irreversibilities and to calculate the specific exergy loss for each component.

➢ System description

At the Institute of Thermal Engineering of the Graz University of Technology, a laboratory prototype of a small-capacity ammonia/water absorption heat pumping unit for heating and cooling purpose has been developed and tested (Moser et. al., 2007).

The heat pump has been designed to operate with cold water temperatures from -10°C to 20°C and cooling water temperatures from 30°C to 50°C. It is indirectly driven by a heat carrier loop (water or thermo-oil) in order to allow the use of different high temperature heat sources. For all heat exchangers – including absorber and generator – standard plate heat exchangers (PHE) have been used. PHEs offer very large heat transfer areas at compact dimensions, thus small temperature differences can be achieved. For purification of the refrigerant a rectification column combined with a dephlegmator which is cooled by the rich solution has been developed.

In a conventional generator, the liquid solution enters the heat exchanger on the top and leaves the heat exchanger at the bottom; the generated vapour flows upwards in counter-flow to the liquid and leaves the heat exchanger on the top. Using a standard plate heat exchanger for the generator the counter-flow of liquid and vapour requires large flow cross sections in order to avoid “flooding” of the heat exchanger. In the modified scheme the liquid and the generated vapour phase flows in co-current flow through the generator and are separated after the generator in the rectification.

The aim of this work is to to identify potential of improvements of the laboratory prototype and investigate the thermodynamic penalty of a co-current flow in the generator compared to a counter-current flow. Therefore a thermodynamic analysis of two different processes has been performed and compared to each other, including both the first and second law of thermodynamics.

In Figure 1 the design and state points of the absorption heat pump cycle for the co-current generator design (left) and the generator section of the counter-current generator design (right) is shown. The process is described hereafter for the co-current generator design (left). Starting at the absorber, the rich solution flows via the solution accumulator (SAC) to the solution pump where the pressure is increased to the high pressure level. Further the rich solution flows to the dephlegmator where it is heated by the refrigerant at the top of the rectification column and to the solution heat exchanger where it is preheated and possibly partly evaporated by the heat from the poor solution before it enters the generator. In the generator the rich solution is partly evaporated by the high temperature heat source.

The two-phase flow leaves the generator and enters the liquid separator (LS) where it separates into liquid (poor solution) and vapour phase (refrigerant). The poor solution flows through the solution heat exchanger via the solution throttle to the absorber. In the solution

throttle it expands to the low pressure level. The refrigerant flows in the rectification column upwards through the stages in counter flow to the liquid fraction (condensed refrigerant).

The vapour leaving the rectification column on the top flows to the dephlegmator where it is partly condensed. The condensate flows back to the rectification column, while the purified vapour streams to the condenser where it is totally condensed by rejecting the heat to the cooling water. After the condenser the refrigerant flows via the refrigerant accumulator (RAC) to the condensate pre-cooler where it is cooled by the refrigerant leaving the evaporator.

After the pre-cooler the refrigerant expands through the refrigerant throttle to the low pressure level and enters the two-phase region and flows further to the evaporator. Receiving the heat from the low temperature heat source the refrigerant evaporates either partly or totally and flows to the condensate pre-cooler where the refrigerant is further evaporated or superheated and flows to the absorber.

At the absorber inlet the refrigerant vapour and the poor solution are mixed in the mixing point (MP). The mixture flows further through the absorber where the refrigerant is absorbed and the heat is rejected to the cooling water.

On the right hand side of Figure 1 the generator section of the counter-current generator design is shown. It is assumed that the liquid and the vapour, flowing in counter-current flow in the generator, are in thermodynamic equilibrium. Except the generator, no other changes have been assumed for the AHP-process.

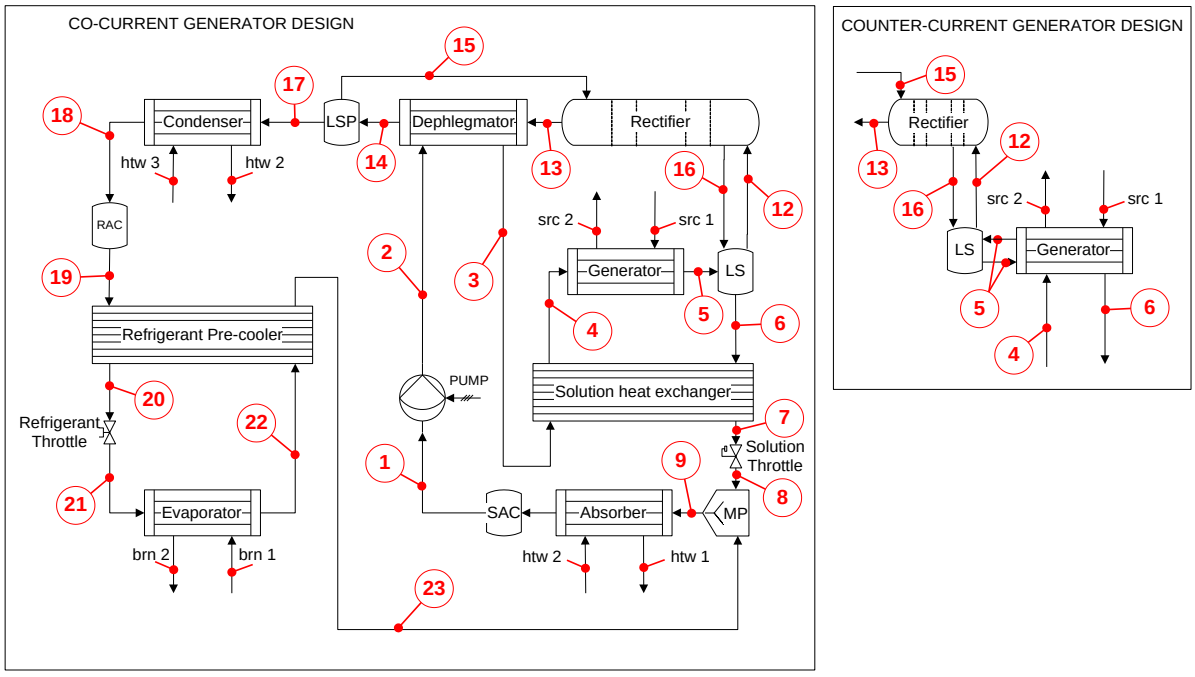

Figure 1 Design and State points of the absorption heat pump cycle for the co-current generator design (left) and the generator section of the counter-current generator design (right)

➢ Used Methodolgy

Two different mathematical models have been developed using the software package EES (2006) in order to study the effects of component behaviors, to perform calculation for

different external heat source and heat sink temperatures, as well as to compare the predictions with the experimental results.

- Fluid Property Data

The thermodynamic properties of ammonia/water mixtures were calculated using the procedure „NH3H2O“ (Ibrahim and Klein, 1993), which is implemented in EES. The external circuits are the cold water circuit for the low temperature heat source, the cooling water circuit for the medium temperature heat sink and the heating water circuit for the high temperature heat source.

For the external circuits, the specific heat capacities are calculated from T_1 to T_2 (at constant pressure) using Eq. 1, the enthalpy differences are calculated using Eq. 2 and the entropy differences are calculated according to Eq. 3 (Lüdecke and Lüdecke, 2000).

$$c_p = a \cdot T^2 + b \cdot T + c \tag{1}$$

$$\Delta h^{1\to 2} = \frac{a}{3} \cdot \left(T_2^3 - T_1^3\right) + \frac{b}{2} \cdot \left(T_2^2 - T_1^2\right) + c \cdot \left(T_2 - T_1\right) \tag{2}$$

$$\Delta s^{1\to 2} = \frac{a}{2} \cdot \left(T_2^2 - T_1^2\right) + b \cdot \left(T_2 - T_1\right) + c \cdot \ln\left(\frac{T_2}{T_1}\right) \tag{3}$$

The used coefficients are given in Table 1. The values for the cold water circuit (brine, 50%$_{Mass}$ Glysantine and 50%$_{Mass}$ Water) are derived from BASF (2001). The values for the cooling water have been determined using the EES-procedure “Water”. For the heating water circuit thermal oil has been considered and the specific heat capacity has been derived from VDI Wärmeatlas (1997) for “BP Transcal N”.

Table 1 Coefficients for the calculation of c_p, Δh and Δs

Description	a	b	c	validity [K]
Cold Water (brine)	-2.4673E-05	2.0468E-02	-0.5101	243 < T < 383
Cooling Water (water)	1.2505E-05	-7.9884E-03	5.4548	273 < T < 423
Heating Water (thermal oil)	0	3.4131E-03	0.9825	273 < T < 590

- First law analysis

For the thermodynamic analysis of the process two steady state models for the co-current and counter current generator design have been set up. The models solve energy, overall mass and ammonia mass balances for all components.

The effect of the rectification process on the water fraction of the refrigerant and on the dephlegmation capacity was calculated using the method of Herold and Pande (1996) (ponchon method), under the assumption of two theoretical plates In order to compare the results, the coefficient of performance for cooling (COP_C) is calculated using Eq. 4. The external temperature lift - which is the temperature difference between the low temperature

heat source and the medium temperature heat sink - is calculated using Eq. 5. $\Delta\xi$ means the concentration difference between the rich solution and the poor solution (Eq. 6). The internal heat exchanger efficiencies (ε) have been considered to be constant acc. to Eq. 7. Where $\dot{Q}_i$ means the actually transferred capacity and $\dot{Q}_{i,max}$ the maximum possible capacity determined by the inlet temperatures.

$$COP_C = \frac{\dot{Q}_{EVA}}{\dot{Q}_{GEN} + P_{PUMP}} \tag{4}$$

$$\Delta T_{LIFT} = \frac{T_{htw;1} + T_{htw;3}}{2} - \frac{T_{brn;1} + T_{brn;2}}{2} \tag{5}$$

$$\Delta\xi = \xi_{rso} - \xi_{pso} \tag{6}$$

$$\varepsilon = \frac{\dot{Q}_i}{\dot{Q}_{i,\max}} = const. \tag{7}$$

In order to solve the system of equations, different assumptions and the definition of boundary conditions for the external circuits are necessary. Table 2 summarizes these assumptions, which have mainly been derived and validated by the recalculation of the process using experimental results of the prototype application.

Beside the temperature differences, the UA-value - which is the product of the coefficient of heat transfer and the heat transfer area - of the dephlegmator has been assumed to be constant and has been calculated using Eq. 8. Because of the fact that the specific heat capacity of the refrigerant along the dephlegmator is not constant the heat exchanger has been subdivided into 10 parts with the same capacity of transferred heat. For each part the specific heat capacity has been assumed to be constant and the thermodynamic mean temperature differences have been calculated using Eq. 9. The average value of these temperature differences has been calculated using Eq. 10 were N is the number of subdivided parts.

$$UA_{DEP} = \frac{\dot{Q}_{DEP}}{\Delta T_{LOG,DEP}} \tag{8}$$

$$\Delta T_{LOG,DEP,i} = \frac{(T_{ref,i} - T_{rso,i}) - (T_{ref,i+1} - T_{rso,i+1})}{\ln\left(\frac{(T_{ref,i} - T_{rso,i})}{(T_{ref,i+1} - T_{rso,i+1})}\right)} \tag{9}$$

$$\frac{1}{\Delta T_{LOG,DEP}} = \frac{1}{N} \cdot \sum_{i=1}^{N} \frac{1}{\Delta T_{LOG,DEP,i}} \tag{10}$$

Table 2 Assumptions and boundary conditions used for the process calculation

State point	Value	Unit	Description
Q_{GEN}	10	kW	Capacity of the generator
m_{brn}	0,35	kg/s	Cold water mass flow rate (brine)
m_{htw}	0,5	kg/s	Cooling water mass flow rate (water)
m_{src}	0,35	kg/s	Heating water mass flow rate (thermal oil)
t_E	17	°C	Temperature of the environment
ΔT_1	4	K	Temperature difference between t_1 and $t_{htw;2}$
ΔT_{1_sat}	2	K	Temperature difference between saturation temp. at point 1 and t_1
ΔT_{18}	4	K	Temperature difference between t_{18} and $t_{htw;3}$
ΔT_{21}	5	K	Temperature difference between $t_{brn;2}$ and t_{21}
ΔT_{GEN}	14	K	Logarithmic mean temperature difference in the generator
$\Delta T_{22\text{-}21}$	6	K	Temperature difference between t_{22} and t_{21}
$UA_{DEP,co\text{-}current}$	200	W/K	UA-value of the dephlegmator for the co-current generator design
$UA_{DEP,counter\text{-}current}$	100	W/K	UA-value of the dephlegmator for the counter-current generator design
q_6, q_{15}, q_{16}, q_{18}	0	-	Vapor fraction at state points 6, 15, 16 and 18
q_{12}, q_{13}, q_{17}	1	-	Vapor fraction at state points 12, 13 and 17
ε_{SHX}	0,88	-	Heat exchanger efficiency of solution heat exchanger
ε_{PRC}	0,5	-	Heat exchanger efficiency of refrigerant pre-cooler
η_{PUMP}	0,5	-	Isentropic efficiency of solution pump

- Second law analysis

According to the first law of thermodynamics all forms of energy are convertible in one another. But different forms of energy have different potential to produce work, thus the second law of thermodynamics limits the possible energy conversion. The second law analysis of the absorption heat pump have been performed by determining the exergy losses of each process component according to Aphornratana and Eames (1995). The procedure is described hereafter.

A reversible process is one that can be reversed completely and after reversing no change remains in the system or its surroundings. All real processes are not reversible due to e.g. friction, heat transfer, hysteresis, mixing or diffusion processes. Exergy is defined as the maximum possible reversible work that can be obtained from a source with respect to the surrounding environment and is given for work in Eq. 11, for heat in Eq. 12, and for a mass

flow in Eq. 13, if changes in the potential and kinetic energy can be neglected. Heat and work interaction can be defined in terms of exergy, which always decreases during real irreversible processes. For each process or component, the exergy loss can be calculated applying Eq. 14.

$$\dot{E}_P = P \tag{11}$$

$$\dot{E}_Q = \left(1 - \frac{T_{ENV}}{T}\right) \cdot \dot{Q} \tag{12}$$

$$\dot{E}_M = \dot{m} \cdot \left[h - h_E - T_E \cdot \left(s - s_E\right)\right] \tag{13}$$

$$\Delta\dot{E} = \sum \dot{E}_P + \sum \dot{E}_Q + \sum \dot{E}_M \tag{14}$$

In the following heat losses to the environment have been neglected and, except in the solution pump, no work is supplied, thus only the mass flows are to be considered according to Eq. 14.

In order to calculate the exergy losses due to the heat transfer it is necessary to calculate a theoretical temperature profile of the external heat sources and heat sinks where the minimum approach temperature in the component is zero. For this theoretical temperature profile the heat transfer area of the component has to be infinite. An example the different temperature profiles in the condenser is given in Figure 2.

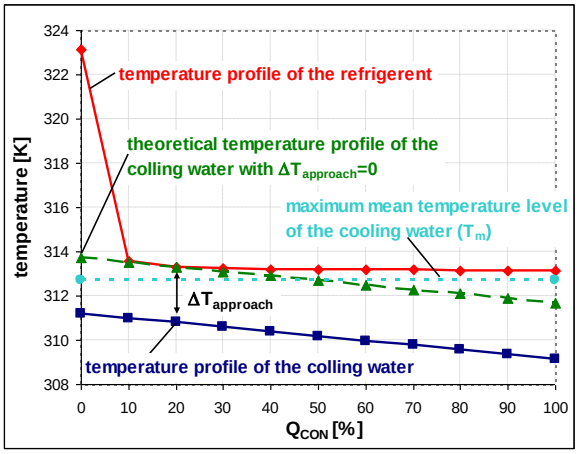

Figure 2 Temperature profile in the condenser and illustration of the minimum approach temperature and the theoretical temperature level of the cooling water

Assuming constant specific heat capacities of the external fluids, the thermodynamic mean temperature level of the theoretical temperature profile can be calculated as shown in Eq. 15. Depending whether the heat is supplied to, or rejected from the absorption heat pumping process by the component, the exergy loss due to the heat transfer is calculated using the Eq. 16 for the generator & evaporator, and using Eq. 17 for the absorber & condenser.

The exergy loss due to internal irreversibilities is the difference between the total exergy loss of the component and the exergy loss due to the heat transfer.

$$T_m = \frac{T_{in} - T_{out}}{\ln\left(\frac{T_{in}}{T_{out}}\right)} \tag{15}$$

$$\Delta\dot{E}_{HT} = \Delta\dot{E}_{c,in} - \Delta\dot{E}_{c,out} - \dot{Q}\cdot\left(1 - \frac{T_E}{T_m}\right) \tag{16}$$

$$\Delta\dot{E}_{HT} = \Delta\dot{E}_{c,in} - \Delta\dot{E}_{c,out} + \dot{Q}\cdot\left(1 - \frac{T_E}{T_m}\right) \tag{17}$$

➢ Results and Discussion

Figure 3 shows the comparison in terms of COP_C , for the co-current generator, between the measured values of the prototype application and those derived from the thermodynamic model (with t_{21} = -10°C, compare Fig. 1, and $\Delta\xi$ = 0.1). The COP_C decreases with increasing temperature lift approximately linearly from about 0.7 at 15 K down to approximately 0.4 at 45 K temperature lift. The thermodynamic model shows a similar characteristic but with approximately 0.05 higher COP_C values compared to the measurements.

Figure 4 shows the COP_C as a function of the generator outlet temperature of the poor solution (t_6) for four different load cases, with evaporation/condensation temperatures of 10/30, 0/30, 10/50 and -10/50 °C and for $\Delta\xi$, varying in the range 0.05-0.15. The temperature of the poor solution at the generator outlet increases from about 70°C to over 170°C and the COP_C decreases from about 0.75 to about 0.4 for the 4 load cases. The deviation of the results between the co-current and counter-current generator (compare Fig. 1) increases with increasing generator temperature whereas the difference is small for a small $\Delta\xi$ and becomes higher with increasing $\Delta\xi$□. The results for the co-current generator show a maximum of the COP_C at $\Delta\xi$ = approx. 0.1 for all load cases while for the counter-current generator the COP_C has a maximum at $\Delta\xi$ > 0.15.

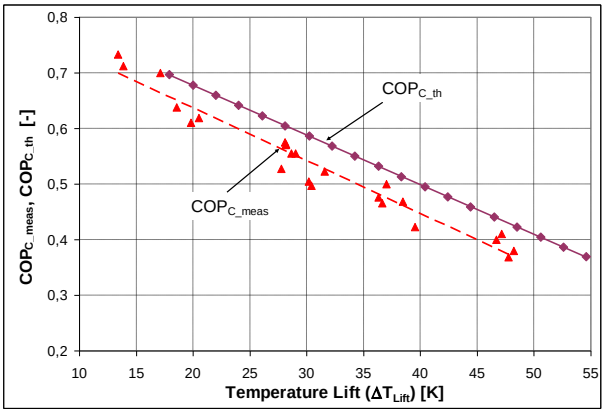

Figure 3 Comparison of the COP_C of the measurements and of the thermodynamic model for the co-current generator design depending on the temperature lift.

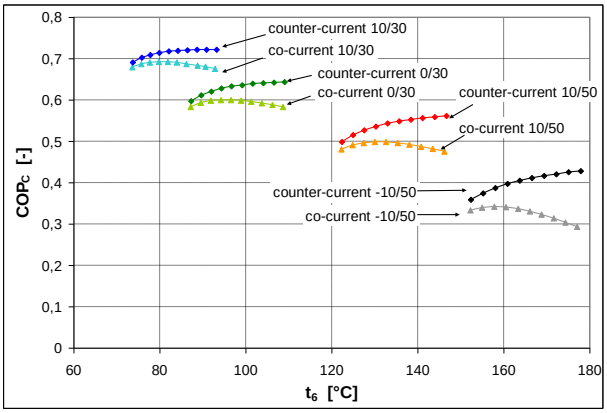

Figure 4 COP_C depending on t_6 for the co-current and counter current flow generator design for four load cases with evap./cond. temp. of 10/30, 0/30, 10/50 and -10/50 °C and varying $\Delta\xi$ = 0.05 to 0.15.

In order to gain a more detailed insight to the origin of the process losses, the exergy loss of each process component has been calculated for both generator designs. Figure 5 shows the simulation results for an evaporation temperature of -10°C and varying condensation temperature (10 up to 50°C) for co-current generator design (left) and counter-current generator design (right). The total exergy loss of the AHP increases for both designs with increasing temperature lift. At a small temperature lift (10 K) both designs have a total exergy loss of about 1.32 kW. At a large temperature lift (50 K) the AHP with the co-current generator design has a total exergy loss of about 1.95 kW and the counter-current generator design of about 1.83 kW.

Comparing the component losses of the two designs,it can be seen that - except the dephlegmator, rectification column and solution heat exchanger - the component losses are very similar. Particular the exergy losses of the dephlegmator and the rectification are significantly higher at high temperature lift for the co-current design. This is mainly caused by the higher temperature and water content of the refrigerant vapour entering the rectification column for the co-current design. Thus also the capacity of the dephlegmator is significantly higher for the co-current design. The exergy loss of the solution heat exchanger is lower for the co-current design. Because of the preheating of the rich solution, in the dephlegmator the solution heat exchanger has a higher capacity for the counter current design, which leads to higher exergy loss.

The exergy losses in the “main” components - which are the absorber, generator, condenser and evaporator - have been divided into one part which originates from the heat transfer and one part which is caused by internal losses. The absorber causes approx. 30% of the total exergy loss at low and high temperature lifts, whereas the internal losses dominate. This is mainly caused by the much higher gradient of the temperature profile in the process flow compared to the gradient of the temperature profile in the cooling water flow. This means that increasing the absorber component size – which affects the exergy losses due to heat transfer - would have a minor effect on the total exergy losses. Lowering the cooling water mass flow rate would decrease the internal exergy losses in order to achieve similar gradients of the temperature profiles in the component. However, this would also increase the mean temperature level of the absorber and influences the losses of other components which maybe decrease the system efficiency.

The generator causes approx. 30% of the total exergy loss of the absorption heat pump at a low temperature lift and approx. 10% at a high temperature lift. Due to the fact that the gradients of the temperature profiles of the rich solution and the thermal oil in the generator are similar to each other, the exergy losses are mainly caused by the heat transfer and can be decreased be increasing the component size or improving the heat transfer. In the evaporator and condenser the absolute value of the exergy losses decrease with increasing temperature lift which is mainly caused by the decreasing component capacity.

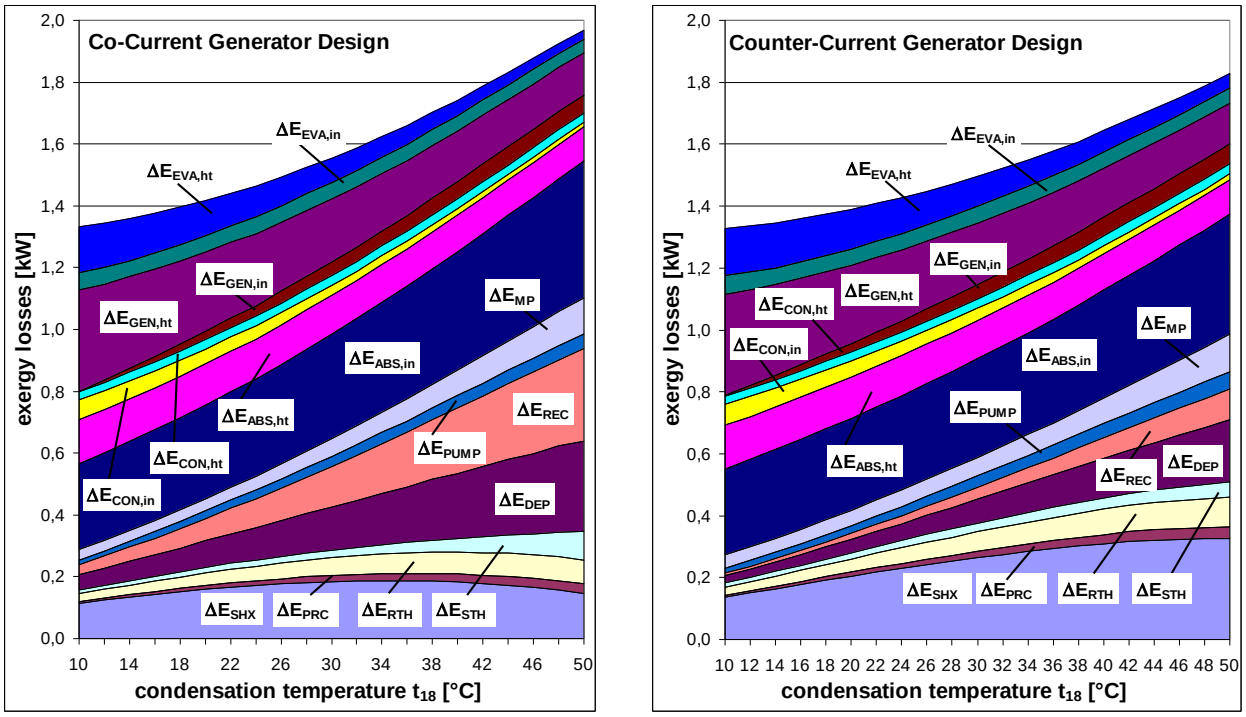

Figure 5 Exergy losses for an evaporation temperature of -10°C and varying condensation temperature (10 up to 50°C) for $\Delta\xi$ = 0.1

➢ Conclusions

A thermodynamic analysis of two single stage NH_3/H_2O absorption heat pumps, with a co-current and a counter-current generator has been presented. As expected, the models show higher efficiencies for counter-current generator design.

The deviation between co-current and counter-current generator design increases with increasing generator temperature and concentration difference between rich and poor solution.

In order to determine the magnitude of the irreversibilities which occur in the different components an exergy analysis has been performed.

The results show that, due to the increased rectification and dephlegmation effort, the exergy losses of these components are significantly higher at the co-current generator design, particular at high temperature lifts. In order to minimize the exergy losses the improvement of the heat transfer in the generator and solution heat exchanger seems to be most promising. Even though the absorber causes approx. 30% of the total exergy losses it has a lower potential for improvement, because only a small part of the component exergy loss can be affected by the heat transfer.

➢ Acknowledgement

This work has been carried out within the IEA SHC Task 38 and is financially supported by the Austrian Federal Ministry for Transport, Innovation and Technology. The authors also wish to thank Daniel Dornstädter who conducted a great part of the experimental investigations and spent a lot of programming effort.

NOMENCLATURE

c_p	Specific heat capacity	[kJ/(kg K)]
$\dot{E}$	Exergy	[kW]
ε	Efficiency	[-]
h	Specific enthalpy	[kJ/kg]
$\dot{m}$	Mass flow rate	[kg/s]
p	Pressure	[kPa]
P	Mechanical power	[kW]
$\dot{Q}$	Thermal capacity	[kW]
q	Vapour fraction	[-]
s	Specific entropy	[kJ/(kg K)]
t	Temperature	[°C]
T	Temperature	[K]
ξ	Ammonia mass fraction	[-]

Subscripts

E	environment	
ext	external	
i	index	
in	inlet	
meas	measurement	based
out	outlet	
th	theoretical model	

brn	Cold water (brine)
htw	Cooling water (water)
pso	Poor solution
ref	Refrigerant
rso	Rich solution
src	Heating water (thermal oil)
ABS	Absorber
CON	Condenser
DEP	Dephlegmator
EVA	Evaporator
GEN	Generator
LS	Liquid separator downstream
LSP	Liquid separator upstream
MP	Mixing point upstream ABS
PUMP	Solution pump
PRC	Condensate precooler
RAC	Refrigerant accumulator
REC	Rectification column
RTH	Refrigerant throttle
SAC	Solution accumulator
SHX	Solution heat exchanger
STH	Solution throttle

REFERENCES

1. Aphornratana S., Eames I. W., 1995, Thermodynamic analysis of absorption refrigeration cycles using the second law of thermodynamics method, *Int. J. Refrigeration*, 18, 4, 244-252
2. BASF, 2001, Glysantin Stoffdaten, *BASF AG D 67056 Ludwigshaven*, ESB/A-J550
3. Boer D., 2005, Structural coefficients in the thermoeconomic analysis of absorption cycles – application to an ammonia-water system, *Int. Sorption Heat Pump Conference Denver, USA*, ISHP-005-2005
4. EES, 2006, Engineering Equation Solver - Vers. 7.693, © 1992-2006 S.A. Klein
5. Fernández-Seara J. Vázquez M., 2001, Study and control of the optimal generation temperature in NH3-H2O absorption refrigeration systems, *Applied Thermal Engineering* 21: 343-357
6. Herold K., E. Pande M., 1996, Counterflow Vapor-Liquid Exchange Processes Using Ammonia/Water, *Int. Ab-Sorption Heat Pump Conference*, *Montreal*, 481-488
7. Ibrahim, O.M., Klein, S.A., 1993, Thermodynamic Properties of Ammonia-Water Mixtures, *ASHRAE Trans.: Symposia*, 21, 2, 1495,
8. Moser H., Rieberer R., Böck M. 2007, Small-capacity ammonia / water absorption heat pump for heating and cooling, *International Congress of Refrigeration 2007, Beijing*.
9. VDI Wärmeatlas, 1997, Berechnungsblätter für den Wärmeübergang, 8. Auflage, *VDI Verlag GmbH,* Düsseldorf, Germany.

On the reference state for exergy when ambient temperature fluctuates (Michel Pons)

- Problem description

Oppositely to entropy, exergy is defined with respect to ambient (outdoor) temperature, in such a way that ambient air is the so-called dead-state; *i.e*. with zero exergy.

This framework does not raise any problem as long as ambient temperature is constant. However, ambient temperature fluctuates, and so does any characteristic of ambient air (pressure, composition, etc.). Now, it must be remarked that some systems or processes are by principle strongly related to ambient temperature and its fluctuations; among them are solar-powered processes, or buildings seen as thermodynamic systems.

For instance, one can think of night ventilation as a means of refreshment, air-to-ground heat-exchangers, or that PCM storage system that one partner of Task-38 (ZAE Bayern) implements between a solar-powered absorption air-conditioner and … ambient air: in all those processes exchanges with ambient air at given periods are for the benefit of the process, when they are not at other moments. In such conditions, can exergy of ambient air be always zero? More generally, can a fluctuating quantity be a reference for defining a thermodynamic function?

There are presently two assumptions. Assumption #1: the reference state for exergy is that defined by the (fluctuating) characteristics of ambient air at any moment (exergy of ambient air always cancels out); Assumption #2: the reference state for exergy is fixed and exergy of ambient air always might cancel out only at very rare moments.

- Analysis

The present analysis consists of exploring both assumptions for two simple problems.

The first concern is thermalization of a given system with ambient air while the temperature of the latter changes. Consider a system with specific heat c_p at temperature T surrounded with ambient air at $T_a(t)$. In the initial state, the system is at T_i, the ambient air at $T_{a,i}$. In the final state, both are at T_f.

- Assumption #1: specific exergy is defined as: $b = c_p\left([T - T_a(t)] - T_a(t).\mathrm{Ln}[T / T_a(t)]\right)$.

The initial value of b can easily be computed, $b_i = c_p\left([T_i - T_{a,i}] - T_{a,i}.\mathrm{Ln}[T_i / T_{a,i}]\right)$; the final value obviously cancels out, so that the exergy change also is given by b_i.

However, in this framework the maximal amount of work (per unit mass) potentially produced by a reversible process operated between that system and ambient air along the thermalization process is given by the integral: $w = c_p \int_{T_i}^{T_f} (1 - T_a(t)/T)\mathrm{d}T$.

It can readily be seen that w depends on the exact evolution of ambient temperature along the process (and not only on the initial and final values). For instance, w is not the same if T_a follows the path 1, or the path 2, or the path 3 (Fig. 17).

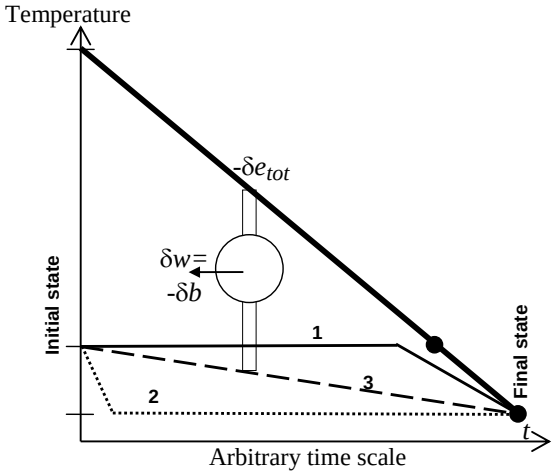

Fig. 17

This difference is essential: the change in the so-defined function *b* only depends on the initial and final states, when the maximal work depends on the respective evolutions along the process. It can thus be said that changes in b have little in common with any maximal produced work.

- Assumption #2: specific exergy is defined as: $b = c_p\left([T - T_0] - T_0.\mathrm{Ln}[T/T_0]\right)$

where T_0 is a reference temperature. This is the usual framework of exergy, with all its usual properties: changes in b do represent a maximal produced work, except that instead of stating that ambient air at $T_a(t)$ always is the *dead-state*, this framework considers only one dead-state, leading then to the notion of ideal heat source at T_0.

The reference temperature can now be defined as the value of ambient temperature (during the period under consideration) which is the most favorable to the process. The most favorable ambient temperature, is the lowest value when the process rejects heat to ambient air, the highest one when the process extracts heat from ambient air (*e.g*. heat-pump). In the case of the Figure above it would be final ambient temperature.

Then, one can imagine an ideal storage implemented between the system undergoing the studied transformation and ambient air: it would be maintained at T_0 (the final value in case presented in the Figure). Rejecting heat to this ideal-heat-storage (instead of to ambient air) obviously increases the process efficiency.

This first problem demonstrates that assumption #1 leads to paradoxes, when assumption #2 does not raise any difficulty and moreover introduces into the analysis the possibility of implementing a heat storage between the process and ambient air.

As second concern, let us study a mechanically-powered air-conditioner operated in a periodically fluctuating ambient air; we will focus on the reversible case. The ambient temperature undergoes a periodic fluctuation, and with it the heat-exchanger that releases heat to ambient air. Consequently, both total energy and total entropy contained in the air-conditioner are likely to fluctuate. In the reversible case, the instantaneous energy and entropy balances write:

$$e_p + q_a + e_u = \dot{E} \quad \text{AND} \quad s_p + \frac{q_a}{T_a} + s_u = \dot{S}$$

The index *p* stands for *power* and the index *u* for *utility*, *E* and *S* are the total energy and entropy contained inside the machine. Like the ambient temperature T_a, all fluxes (*e*, *q*, *s*) fluctuate periodically (the process has reached the periodical regime).

- Assumption #1: exergy is defined as: $b_x = b_x - T_a(t).s_x$,

where the index *x* can be *p* or *u*. If this function exergy is integrated over the cycle period, then the difference between the *power* exergy (B_p) and the *useful* one (B_u), does not cancel out in general. This integral remains in the balance: $\int T_a \dot{S} \mathrm{d}t$. This quantity is unknown in thermodynamics, and it can be positive or negative depending on the respective evolutions of S and T_a. It cannot be interpreted as an exergy loss. As a consequence, in the framework of assumption #1, it can no longer be said that a reversible process delivers as much exergy as it receives. Can still rational exergy analyses be developed?

- Assumption #2: exergy is now defined with a fixed reference according to: $b_x = b_x - T_0.s_x$,

where the index *x* can be *p* or *u*. The dead-state is fixed and does not fluctuate, oppositely to ambient air. The exergy of ambient air does not cancel out (in general). Now, integration of the above-given balances results in another integral: $\int -q_a(T_0^{-1} - T_a^{-1})\mathrm{d}t$.

When the reference state is defined like in the former problem, this integral is always positive, may cancel out (if T_a always T_0), and can be interpreted as an exergy loss, that due to the rejection of q_a toward ambient air instead of the ideal heat-storage as defined above.

Now, any reversible process can exactly deliver as much exergy as it receives, as soon as it is equipped with an ideal heat-storage that remains at the temperature level given by the most favorable value of ambient air during the period. In the case of non-reversible process and non-ideal heat-storage, the exergy losses due to non-ideality of heat-storage can be pointed out, evaluated and added to those generated in the process itself. Now the whole process can be globally optimized.

➢ Conclusion

Also when ambient temperature fluctuates, exergy must be defined with respect to a constant dead-state, as much for the state where exergy cancels out as for the temperature value in factor of entropy. This constant temperature must be the value of ambient temperature which is the most favorable to the process along the period under consideration.

When extending the analysis to other physical characteristics of ambient air, it can be seen that the dead-state should be the composite of all the most favorable values of any characteristic.

In this framework, exergy of ambient air is almost never zero, but processes like heat-storage between night and day, or between winter and summer, can be analyzed rationally in terms of exergy as a component of a global process which now can be optimized.

➢ Bibliography

- Pons M., Bases for second law analyses of solar-powered systems, Part 2: the external temperature, *ECOS-2008 21st Int. Conf. on Efficiency, Cost, Optimization, Simulation & Environmental Impact of Energy Systems*, Cracow-Gliwice, Poland, 24-27 June 2008, A. Ziebik, Z. Kolenda & W. Stanek Ed., Pub. AGH Univ. Sci. Technol., ISBN 978-83-922381-4-0, Vol. 1, pp. 147-154, 2008.
- Pons M., On the refererence state for exergy when ambient temperature fluctuates, *Int. J. of Thermodynamics*, **12(3)**, pp. 113-121, 2009.
- http://www.limsi.fr/Individu/mpons/Pons_IJoT2009_web.pdf